UNIVERSITY OF TARTU

Faculty of Science and Technology

Institute of Physics

Umama Quddusi

Investigation of luminescence properties of Pr^{3+} doped $LaPO_4$ micro- and nanopowders

Material Science and Technology

Master's Thesis (30 ECTS)

Supervisor: Prof. Marco Kirm

Laboratory of Physics of Ionic Crystals

Institute of Physics

University of Tartu

Tartu 2022

Investigation of luminescence properties of Pr^{3+} doped $LaPO_4$ micro- and nanopowders

Abstract:

The main goal was to investigate potential scintillation materials, which would help to increase the efficiency of radiation therapy for cancer treatment via emitting UV-C locally in patient's tissue. For this purpose, the relaxation processes of electronic excitations in Pr^{3+} doped $LaPO_4$ micro- and nanopowders were investigated using cathodoluminescence and VUV photons. The luminescence properties of the $LaPO_4$:Pr^{3+} nanoparticles were compared with micro powders which represent behaviour of the substance in bulk form. Taking advantage from high quality synchrotron radiation excitation in VUV some intrinsic properties of studied materials were evaluated using luminescence spectroscopy. Cathodoluminescence results were analysed considering the morphology of Nano samples obtained by transmission electron microscopy. The investigated nanopowders consist of nanofibers with thicknesses of few nm and lengths varying from 20 to a few hundred nm.

For all micro and Nano samples the luminescence, spectrally located between 5.8 to 4.4 eV, of Pr^{3+} ions due to $4f^15d^1 \rightarrow {}^3H_{4,5,6}$ and ${}^3F_{2,3}$ interconfigurational transitions were revealed. At low temperatures self-trapped exciton luminescence at 4.7 eV was observed in micro and Nano samples when excited in the $LaPO_4$ host absorption (> 8.2 eV). The final stages of the scintillation process were studied using luminescence spectroscopy under VUV excitation using FinEstBeAMS beamline at MAX IV Lab. The onset of multiplication process of electronic excitations, forming two electron-hole pairs in $LaPO_4$, is at 18 eV, which well visible in Nano samples. The results on 5d-4f of Pr^{3+} ion luminescence of this research is a valuable contribution to the development of Nano scintillators for various medical applications.

Keywords: scintillators, radiation therapy, Pr^{3+} doped $LaPO_4$, micro and Nano powder, 5d-4f and 4f-4f emissions, self-trapped exciton, luminescence spectroscopy, cathodoluminescence

CERCS: P260 Condensed matter: electronic structure, electrical, magnetic and optical properties, superconductors, relaxation, spectroscopy; T151 Optical materials

Pr^{3+} lisandiga $LaPO_4$ mikro- ja nanopulbrite luminestsentsomaduste uurimine

Lühikokkuvõte

Töö peaeesmärgiks oli uurida potentsiaalseid stsintillaatormaterjale, mille abil on võimalik suurendada kiiritusteraapia efektiivsust vähiravis viies neid materjalid patsiendi kehasse, kus need kehas lokaliseeritult kiirgavad UV-C piirkonnas mõjutades kasvajarakke. Kasutades katoodluminestsentsi ja footoneid VUV piirkonnas uuriti elektronergastuste relaksatsiooni Pr^{3+} lisandiga $LaPO_4$ mikro ja nanopulbrites. Pr^{3+} lisandiga $LaPO_4$ nanopulbrite luminestsentsomadusi võrreldi mikropulbrite vastavate omadustega ning viimased esindavad materjali omadusi makro (tahkise) olekus. Kasutades suurpärase kvaliteediga sünkrotronkiirgust VUV piirkonnas uuriti samuti $LaPO_4$ põhiaine mõningaid omadusi luminestsentsspektroskoopia meetoditel. Katoodluminestsentsi uuringutulemusi analüüsides võeti arvesse nanopulbrite morfoloogia, mis määrati kindlaks läbivalgustava elektronmikroskoopia abil. Uuritud nanopulbrid koosnevad nanofiibritest, mille paksus on mõned nanomeetrid ja pikkus varieerub 20 kuni mõnesaja nanomeetrini.

Kõikides mikro ja nanopulbrites leiti Pr^{3+} iooni $4f^15d^1 \rightarrow {}^3H_{4,5,6}$ and ${}^3F_{2,3}$ elektronkonfiguratsioonide vahelistest üleminekutes tingitud kiirgused 5.8 ja 4.4 eV spektraalpiirkonnas. Madalatel temperatuuridel kiirgab iselõksustunud eksiton 4.7 eV juures kui ergastada $LaPO_4$ tema omaneeldumise piirkonnas (> 8.2 eV). Stsintillatsioonis aset leidvaid protsesse uuriti FinEstBeAMS kiirekanalil MAX IV Laboris (Lund, Rootsi) kasutades selleks luminestsentsspektroskoopiat VUV ergastusel. Elektronergastuste kordistumise protsess algab 18 eV juures kui üks footon tekitab kaks elektron-auk paari. See lävi on eriti hästi näha nanopulbrites. Saadud uuringutulemused Pr^{3+} 5d-4f luminestsentsi kohta on väärtuslik panus nanostsintillaatorite arendamisse erinevate meditsiini rakenduste jaoks.

Võtmesõnad: stsintillaatorid, kiiritusteraapia, Pr^{3+} lisandiga $LaPO_4$, mikro ja nanopulber, 5d-4f ja 4f-4f kiirgused, iselõksustunud eksiton, luminestsentsspektroskoopia, katoodluminestsents

CERCS: P260 Tahke aine: elektrooniline struktuur, elektrilised, magneetilised ja optilised omadused, ülijuhtivus, magnetresonants, spektroskoopia; T151 Optilised materjalid.

Table of Contents

Abbreviations

UV	Ultraviolet
UV-VIS	Ultraviolet-Visible
VUV	Vacuum Ultraviolet
IR	Infrared Radiation
DNA	Deoxyribonucleic Acid
NCs	Nano crystals
PL	Photo Luminescence
IRF	Instrumental Response Function
XRD	X-Ray Diffraction
TEM	Transmission Electron Microscopy
E_g	Energy Gap
e-h	Electron-Hole
SR	Synchrotron Radiation
STE	Self-trapped exciton
PAW	Project Augmented Wave

1: Introduction

Globally cancer is a vital cause of mortality, and million new medical cases and deaths are characteristic to malignant tumor [1]. Although, rapid advances have been made in lesion diagnostic procedures and treatments but the overall survival rate from such disease has not yet significantly improved. Many treatments and noninvasive methods for imaging and cancer treatment are being studied and developed that would have minimal possible side effect to the investigated systems and organs. At present, 50% patients receive radiation therapy during the scheduled treatment of this disease [2]. Although radiation therapy is promising and effective treatment of cancer patient targeting highest doses of radiation to the affected area with minimal damage to the surrounding but also carry toxic side effects.

To minimize the risk of toxic side effects efforts are being made for the optimization in the current radiation therapy techniques by research and development in inorganic scintillators to yield synergistic effect between ionizing (X-rays) and UV-C radiations against cancer cells. Whereas a scintillator is kind of luminescent material that work as an energy transformer, their function is to convert high-energy X- and γ-rays as well as high energy particles into lower-energy ultraviolet (UV) and visible (Vis) lights (400–700 nm), where exist fast and efficient photodetectors. Main applications of such materials include medical imaging, photodynamic therapy, security, well logging and high energy physics. In enhancement of radiation therapy for cancer treatment, these UV-emitting scintillators *e.g.,* $LaPO_4$ doped with praseodymium Pr^{3+} are beneficial because photons will be generated locally in the region of lesions and influence tumors at cellular level. The Pr^{3+} ions yield broad band emissions in UV-C range due to interconfigurational $4f^15d^1$-$4f^2$ transitions [3]in the spectral region where, DNA has its absorption bands from 200-300 nm [4]. These UV-C photons will influence tumor's DNA directly via cell interaction with free electrons as well as free radical and reactive oxygen species formed during therapy, which will ultimately reduce metastasis survival rate in hypoxic regions within tumor. Also, the plight of low penetration depth of UV-C radiations generated by scintillators in Nano-scale will significantly improve treatment inside tumor and simultaneously protecting nearby tissues from harmful radiations [5]. Nanoscale particles are of interest because of their small size, these particles can

penetrate through various tissues and their larger surface area-to-volume ratio also improves surface binding. Additionally, due to their small size they can travel via blood stream and targeted to lesion sites when bound to specific complexes targeting cancer cells.

This master thesis is focused on the development and experimental studies of Nano- and micro powders of $LaPO_4$ doped with praseodymium Pr^{3+} ions, which will have the capability to absorb x-ray and convert high-energy radiation into UV-photons (scintillation). A special attention is paid to the characterization of luminescence properties of Pr^{3+} ions in various excitation regimes.

Nano-particle size effect will be also studied for better understanding of the processes limiting the efficiency of such scintillators and how the relaxation of electronic excitation will occur such low-dimensional materials under VUV excitation in comparison with micropower representing behavior of bulk materials.

The present Master thesis has been prepared in collaboration with several other research groups, who provided Pr^{3+} doped $LaPO_4$ micro- and nanopowders prepared by a suspension method (Prof. Dr. Thomas Jüstel group, Münster University of Applied Sciences,) and a microwave assisted hydrothermal method (Dr. Yury Orlovskiy, University of Tartu and his collaboration network). The main aim of the work is:

- To investigate the relaxation processes of electronic excitations in $LaPO_4$: Pr^{3+} micro- and nanopowders using time-resolved luminescence spectroscopy under synchrotron radiation excitation and cathodoluminescence.
- To investigate in detail the transfer of absorbed energy to emission centers at various excitation regimes: interconfigurational 4f-5d excitation of Pr^{3+} ions; under formation of excitons and electron hole pairs; under multiplication of electronic excitations by higher energy photons. To determine important characteristic parameters for luminescence such as emission wavelength, decay time at different excitation regimes for $LaPO_4$: Pr^{3+} micro- and nanopowders.
- To compare how intrinsic and extrinsic Pr^{3+} 5d-4f emissions behave in micro and nanomaterials.

2: Literature Review

2.1: Luminescence Pr^{3+} Ions in different host materials and conditions for appearance of 5d-4f emissions

Rare earth elements are also often referred to as lanthanides. They are characterized by incompletely filled 4f shells, whereas 4f orbital lies inside the ion, screened by filled $5s^2$ and $5p^6$ orbitals from the surrounding so the influence of host lattice in optical transitions within $4f^n$ configuration is essential but small. There are two types of Inter-configurational transitions in rare-earth ions i.e., charge transfer transition ($4f^n$-$4f^{n+1}L^{-1}$) and $4f^n$-$4f^{n-1}$5d transitions [6]. Over the last few years, the research regarding vacuum ultraviolet VUV spectroscopy of trivalent rare-earth ions (Ln^{3+}) has intensified due to the development of advanced luminescent materials [7]. These lanthanides have widespread applications from laser physics to molecular biology concerning light emissions, for instance, conventional television, and computer screen utilize lanthanide-doped phosphors for converting cathode rays into visible data. Also, they are used as indispensable light amplifying constituents in solid state lasers (*e.g.*, Nd^{3+}: YAG lasers) and in medical diagnostics for studying the physiological state of the patient [8].

Recently there has been an increased interest in study and research regarding Pr^{3+} 5d-4f emissions in wide bandgap hosts [9]. These investigations are devoted to praseodymium-doped compounds because Pr^{3+} intraconfigurational ($4f^2$ -$4f^2$) and interconfigurational ($4f^15d^1$ -$4f^2$) emission transitions have wide applications in lightning, display, health care, and security. Investigation regarding characteristics features of "host lattice-Pr^{3+} "interactions can lead to the development of new materials for scientific applications. Also, the host lattices that assist $Pr^{3+}4f^1$ $5d^1$ -$4f^2$ emission transition have numerous applications in fast scintillators. [10]

In order to implemented Pr^{3+} ions emissions efficiently in various technologies, it is important to understand how the "host lattice-Pr^{3+} "interactions govern the appearance of various types of emission. Such analysis has been summarized by Srivastava in Ref. 10 based on many years' investigation by researchers around the globe.

Depending on crystal field strength of the host material the position $4f^15d^1$ level can be energetically in very different position. The highest $4f^2$ level is $^1S_0$, which determines the possible

relaxation channels following $4f^2 \rightarrow 4f^15d^1$ excitation by any kind of excitation. Figure 1 is reproduced from [10] and it depicts three possible relaxation schemes of the energy absorbed by Pr^{3+} ion or transferred to Pr^{3+} ion after energy absorption by host material.

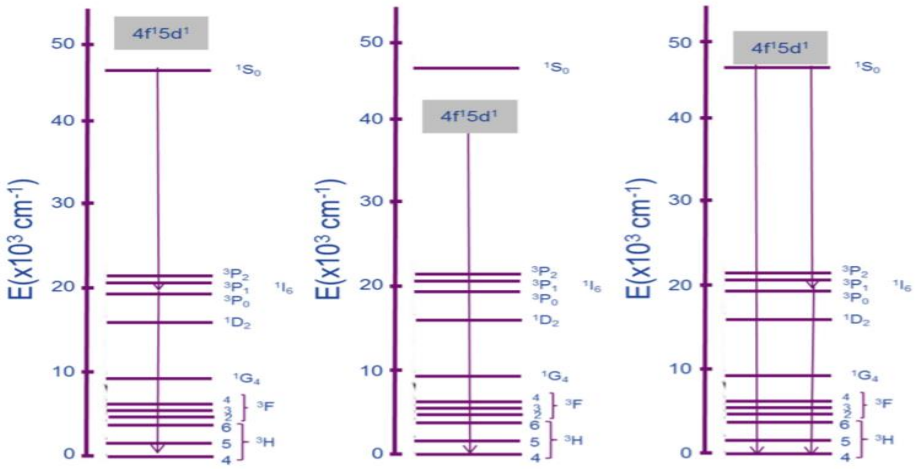

Fig.1: The energy of Pr^{3+} $4f^15d^1$ configuration to the $4f^2$ $^1S_0$ level: (1) $4f^15d^1$ is above the $^1S_0$ level E; $4f^15d^1 > E; {}^1S_0$), (2) $4f^15d^1$ is below the $^1S_0$ level E; $4f^15d^1 < E; {}^1S_0$ and (3) $4f^15d^1$ is close to the $^1S_0$ level E; $4f^15d^1 \approx E; {}^1S_0$. For simplicity only single transition from $^3P_0$ level is shown for the second photon cascade emission step and one $4f^15d^1$ transition only to the ground state $^3H_4$. Adapted from [10].

$Pr^{3+}4f^1\ 5d^1$ configuration is energetically above the $^1S_0$ level

The host lattices support luminescence from $^1S_0$ level, where the energy condition $E; 4f^15d^1 > E; {}^1S_0$ is fulfilled. The left scheme in the Fig. 1 corresponds to such situation. Through the photon cascade emission process [11], it can generate more than one visible photon for each incident UV-VUV photon. The incident vacuum ultraviolet (VUV) photon is strongly absorbed due to parity and spin allowed transitions of Pr^{3+} ions from its ground state (the lowest $4f^2$ $^3H_4$ state) into the excited $4f^15d^1$ configuration. The nonradiative transition from excited $4f^15d^1$ populates the $^1S_0$ level. The photon in the first photon cascade emission step is generated by $^1S_0 \rightarrow {}^1I_6$, ^3P_J and $^1S_0 \rightarrow {}^1D_2$transitions. The second emission step occurs from the lowest $^3P_0$ state to $^3P_0$ as well as from $^1D_2$ to the lower lying $4f^2$ ^3F_J, ^3H_J and ^3H_J levels, respectively. For example, 0.1% Pr^{3+} in YF_3 emits 1.4 visible photon per incident 185 nm vacuum ultraviolet photon [10]. The photon cascade emission has been considered to be useful for lightening applications, but energetically it still inefficient in comparison with common fluorescence tubes.

$Pr^{3+}4f^1\ 5d^1$ configuration is energetically below the $^1S_0$ level

Under specific circumstances Pr^{3+} emission is dominated by broad, parity allowed $4f^15d^1 \rightarrow 4f^2$ interconfigurational transitions when lowest energy component of $Pr^{3+}4f^1d^1$ configuration is located below the $^1S_0$ level (E; $4f^15d^1 < E$; $^1S_0$). It happens when the host crystal field is strong enough to promote significant crystal field splitting in order to obtain that the first $4f^15d^1$ is the lowest electronic state, where radiative transition take place into $4f^2$ states. The scheme in the center of the Fig. 1 corresponds to such situation. As discussed earlier, host lattices that facilitate $Pr^{3+}4f^15d^1 \rightarrow 4f^2$ emissions can be beneficial for development of fast scintillators. But all Pr^{3+} activated host lattices that satisfy the aforementioned condition are not able to support efficient $Pr^{3+}4f^1\ 5d^1$ -$4f^2$ emission transitions. There are two main reasons behind this under performance of these hosts. Namely, not all $4f^15d^1$ transitions terminate in the $4f^2$ ground state, but populate higher lying $4f^2$ levels like $^1I_6$ and $^1D_2$. The same might happen due to the nonradiative relaxation of the excited $4f^15d^1$ level into the lower $4f^2$ (^3P_J, $^1I_6$, $^1D_2$) levels of the Pr^{3+} ion. The harmful influence rises from the circumstance that these $4f^2$ levels emit slow and narrow line intraconfigurational emission, being useless for scintillation purposes [10].

$Pr^{3+}4f^1\ 5d^1$configuration is energetically close to $^1S_0$ level

Since there are very different host materials available, the situation may occur that luminescence from the $4f^15d^1$and $^1S_0$ levels is feasible at the same time. If the lowest energy level of the $Pr^{3+}4f^15d^1$ configuration is located near the $^1S_0$ level satisfying (E; $4f^1\ 5d^1 \approx E$; $^1S_0$) condition. Depending on the energetic distance inter and intraconfigurational emissions may exist simultaneously in certain temperature range. Since the decay times of the emissions are different as well as their luminescence and excitation spectra, the relaxation processes can be conveniently spectroscopically studied as shown in [12]. $LaPO_4$ and $LiLaP_4O_{12}$ are prime examples of the hosts where luminescence from the $Pr^{3+}4f^1\ 5d^1$ and $^1S_0$ levels coexists [10, 12].

2.2: Multiplication of electronic excitations– Creation of secondary excitons and electron-hole pairs by hot photoelectrons

In the scintillation process, energy conversion take place resulting in light (low energy photon) emission when an ionizing particle or photon with much higher energy interacts with matter. These high-energy photons and particles can be in the range of some KeV to MeV of energy and their absorption leads to complex relaxation processes resulting in the emission of several photons having a magnitude of few eV. In the UV-visible range there are highly efficient photodetectors - photomultipliers - with very good time resolution needed in detection of photons emitted by scintillators whereas for detection of high-energy photons and particles situation with various kind sensors is not so favorable.

When these incident photons or particles interact with solid, ionization takes place which generates a hole in the outer core bands or inner core levels and a highly excited hot electron in the conduction band. The probability of interaction of electrons with particles and quasiparticles for instance electrons, plasmons, excitons and phonons, are governed by energy loss function, which is an intrinsic property of the material and represented by:

$$-I_m(1/\varepsilon)$$

where ε is the complex dielectric permittivity of the material.

In the left panel of Fig.2 (adapted from Ref. 16) demonstrates a descriptive sketch of processes governed by the energy loss function. It shows elementary excitations formed after absorption of quanta with different energies and resulting in creation of phonons, excitons, electron-hole pairs and core excitons. Also, the inelastic scattering of hot photoelectrons can produce secondary electron-hole pairs and excitons. Finally, the host lattice vibrations – phonons - participate in the thermalization of excitations bringing electrons to the bottom of conduction band and holes to the top of valence bands. The scattering process of hot photoelectrons (holes), typically created by VUV photons ($h\gamma$) > 2Eg, leads to the multiplication of electronic excitations, which may result in emission of several photons and therefore is called also photon multiplication [13]. Secondary excitons and electron – hole pairs can excite luminescence centers by energy transfer whereas hot photoelectrons can excite impurity centers by impact mechanism as shown

for Tl^+ ions in alkali halides [14]. Photon multiplications processes have been analogously analyzed for $LaPO_4$: Eu and $LaPO_4$: Pr nanoparticles [15.] In most cases created holes relax via Auger decay, resulting finally in production of holes in the valence. The main quantity describing the scintillation process is β, which represents the number of created electron-hole pairs [16];

$$\beta=E_\gamma/(aE_g)$$

where E_γ is the energy of gamma quantum, E_g is energy gap value of the host material and a estimate all energy losses occurring during the relaxation process. The value of a is typically in the range of 1.5 to 3 depending on material.

If each electron-hole pair emits a photon when β represents the theoretical limit of scintillation yield. There are several factors that affect this scintillation yield limit value. For example, when photoelectron energy is below $2E_g$, due to energy and momentum conservation rules [13] it does not generate additional electron-hole pairs and absorbed energy is spent on heat production (i.e., generation of phonons). Also, non-radiative relaxation processes at competing centers (defects, impurities) centers also contribute to losses in scintillators as well as quenching due to the effects caused by high excitation density. [16]

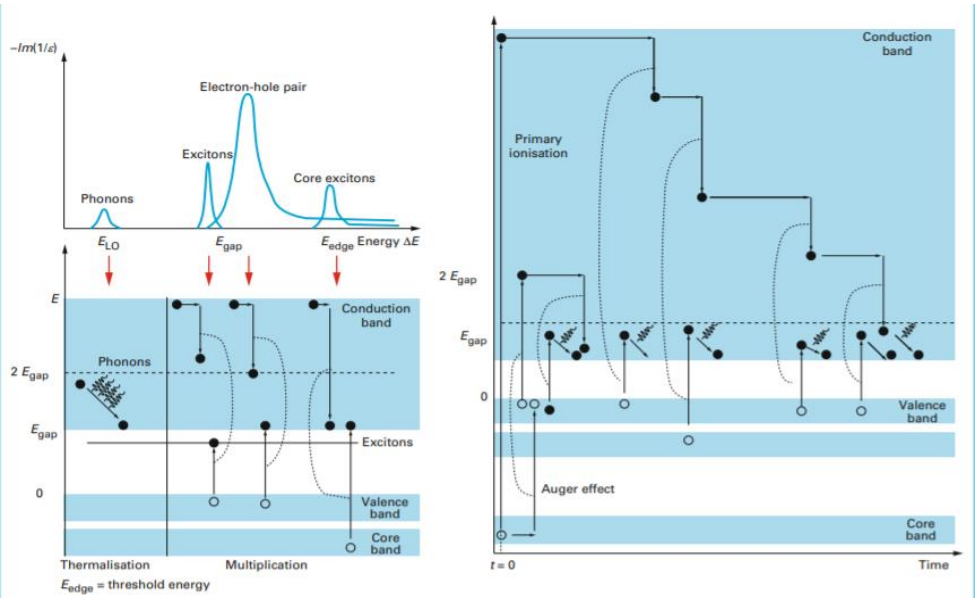

Fig.2: Vibronic and electronic excitations in wide gap solids and their relaxation processes taking place after excitation scintillator by high-energy photon or particle [16]

2.3: Host materials for scintillators

A large number of solids whether crystalline or amorphous can be used as host lattice to incorporate required activator ions in which centers can emit light efficiently [17]. The choice of host matrix depends upon the desired specifications of scintillator. On account of excellent multicolor luminescent properties, high thermal and chemical stability, resistance to radiation and low solubility in water categorize various orthophosphates as a vital host material for doping of trivalent lanthanide ions. It is also reported in the literature that rare earth orthophosphates host lattice can integrate various trivalent lanthanide ions in various concentrations without influencing crystalline structure at high concentrations. Moreover, rare earth orthophosphates have vast applications in luminescent devices as catalysts or labels for biological detection. Also due to their excellent biodegradability and biocompatibility, they are used in several medical applications as well [18]. Due to the exceptional electronic, magnetic, and optical properties namely wide bandgap, high density, and simple crystal structure $LaPO_4$ is considered as an excellent host material for scintillation.

$LaPO_4$

Studies related to the luminescent properties of $LaPO_4$ have gained popularity due to the workability of $LaPO_4$ and its resistance to atmospheric influence. $LaPO_4$ has a number of applications as a host matrix for other lanthanide ions for their use as luminescent biomarkers, radiation storage compounds, photovoltaic and photo-catalysis, and optical devices. $LaPO_4$ in pure and doped form occurs as a monazite monoclinic (M) and hexagonal (H) crystalline phase as shown in Fig. 3 [19]. M-$LaPO_4$ has $P2_1/n$ symmetry and H-$LaPO_4$ acquires $P6_222/n$ symmetry. In M-$LaPO_4$, one-unit cell is dominated by four formula units in which La atoms are nine-fold coordinated (La-O). Out of nine La-O bonds, four oxygen atoms are distorted tetrahedron (PO_4) which permeates a planer pentagon produced by the other five oxygen atoms. H-$LaPO_4$ occurs as a xenoite structure having three formula units per unit cell, in which La atoms are eight-fold coordinated (La-O) and similar to m-$LaPO_4$, four of the oxygen atoms of H-$LaPO_4$ form distorted tetrahedron [19]. The theoretical calculation of the band structure of $LaPO_4$ crystal having monoclinic and hexagonal symmetry was performed by S.V. Syrotyuk *et al*., using the projector

augmented wave (PAW) formalism and the reported band gap value for M-$LaPO_4$ was 6.4eV and 5.9eV for hexagonal symmetry [20]. In Ref. 19 the respective direct energy gap values for M-$LaPO_4$ and H-$LaPO_4$ obtained were 7.82 and 7.30 eV, respectively. The latter value (7.82 eV) are in good agreement with onset of host absorption as shown in the experimental study of M-$LaPO_4$ powders by Nakazawa and Shiga [21]. According to the recorded luminescence excitation spectra and diffuse reflection spectra in the vacuum ultraviolet region 120-300 nm and the revealed energy gap value for $LaPO_4$ is 7.749 eV [21]. The first principle calculation of the band structure reported by K.C Mishra et al., resulted in the band gap value 7.4 eV, which indicates that the energy gap value obtained strongly depends on the quality and approach of theoretical calculations used [22].

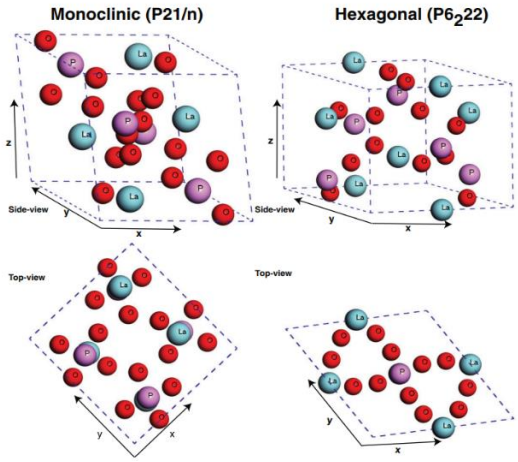

Fig.3: Crystal structure of monoclinic and hexagonal $LaPO_4$. Top-row illustrates the side-view and bottom row illustrates top-view of the primitive cells. Blue, purple, and red balls represent La, P, and O atoms, respectively. **(ref.19)**

2.4: Electronic Properties of Micro to Nano size materials

Particle size reduction plays a significant role in the modification of properties of electronic excitations in a crystalline system due to the high surface-to-volume ratio and quantum confinement effect of nanosized material [23]. It is worthy to note that lanthanide-doped nanocrystals (NCs) have potential applications in the field of bioimaging, Nano thermometry, and luminescent solar concentrators. These NCs vary from their bulk coordinates due to their large surface-to-volume ratio because large number of atoms are located near the surface. Usually, optical properties are expected to be independent of the particle size for lanthanide ions due to the shielding of 4f orbitals by outer filled 5s and 5p orbitals to suppress the impact of local surroundings on the inner $4f^n$ transitions of lanthanides [24]. However, a small but significant influence arising from nanosized is probable. The absorption of photon results in formation of photoelectron with some kinetic energy. If the free mean path of such electron exceeds the size of nanoparticles, the energy will be transferred to the surface of particles and non-radiative relaxation can occur.

It is also reported in the literature that nanoscale phosphors have lower quantum efficiencies as compared to microscale particles because their large surface area, which is responsible for the amplification of the various quenching processes. V. Pankratov *et al.*, studied luminescence properties of bulk and nanosized $LaPO_4$: Ce, Tb, and YVO_4: Eu phosphors under excitation by pulsed vacuum ultraviolet synchrotron radiation in the range of 4.7- 40eV. Their results show a significant difference in emission and excitation spectra of nanoscale versus bulk materials. Their findings indicate that electron-hole pairs and non-radiative annihilation at the surface restrict the energy transfer processes from host lattice to impurity ions [25].

3: Experimental Methods and Materials

The subject of my master thesis is the experimental investigation Pr^{3+}-doped $LaPO_4$ as UV-C emitter to be applied as Nano scintillator in radiation therapy in medicine. My experimental contribution was in cathodoluminescence experiments, which were performed by myself in the laboratory of Physics. Synchrotron radiation research on these materials by photoluminescence spectroscopy was carried out by colleagues from our research team together with staff of the MAX IV laboratory in Lund, Sweden. My master studies took place during the Corona time, which limited access of external users to MAX IV Lab was blocked for considerable time. My contribution to the investigations preformed in Lund was data treatment and analysis as well its graphical presentation.

Cathodoluminescence is a widely used technique for luminescence studies of wide gap crystals. In cathodoluminescence studies an electron beam of few keV either pulsed or stationary is used to excite the material under examination. It allows to investigate luminescence from IR to VUV range, being restricted by energy gap of the material. It is one of the powerful tools for studying radiative processes with low quantum yield. But it has a disadvantage of sample charging in case of insulators as the scintillators are and energetic electrons that may cause radiation damage of the samples investigated. Thus, there are several factors to be considered in the data analysis and these circumstances making it complicated. This is not a highly selective method as photoexcitation, because primary electron beam produces low energy secondary electrons that could excite all possible levels, making it an inappropriate method for identification of specific excitation mechanism.

Synchrotron radiation (SR) excitation has multiple excellent properties in comparison to the experimental setups typically available in the home laboratories using ordinary excitation sources. Charged particles (electrons or positrons) moving at the relativistic velocity with acceleration give rise to SR. It is powerful pulsed light source extending continuously from the IR to X-Ray region. It is superior light source because of providing: 1) strong intense radiation in a wide energy range; 2) SR has a very small source size generating is strongly collimated radiation, which can be focused into spot size of tens of nanometers; 3) SR is polarized and has pulsed nature (~100 ps pulse width) enabling the time resolved studies [26].

3.1: Cathodoluminescence Setup

All $LaPO_4:Pr^{3+}$-doped samples were studied by cathodoluminescence methods. Samples were excited by 10 keV electron beam, with typical 0.5 μA current. The setup is shown in Fig. 4 and described in Ref. [27] Cathodoluminescence setup with our own design at the Institute of Physics, Tartu is stocked with a vacuum cryostat for studying luminescence phenomena in wide range of temperature (5-400 K) including thermoluminescence induced by electron beam irradiation at low temperatures. It is equipped with two monochromators for simultaneous recording of emission spectra in the UV-Vis and VUV range. The first one ARC spectraPro 2300i monochromator with different gratings operates in the range of 200 -1000 nm using various detectors (Photomultipliers and a CCD camera). The self-made double vacuum monochromator equipped with a solar-blind Hamamatsu photomultiplier R6836 covers the wavelength range 120-270 nm. The electron gun used (Kimball Physics EGG-3101) could be utilized in steady and pulsed (10 ns pulse, repetition rate 5 KHz) operation mode. Through the window of sample chamber of cryostat, the visible luminescence can be observed for well emitting samples by naked eye during excitation by electron beam.

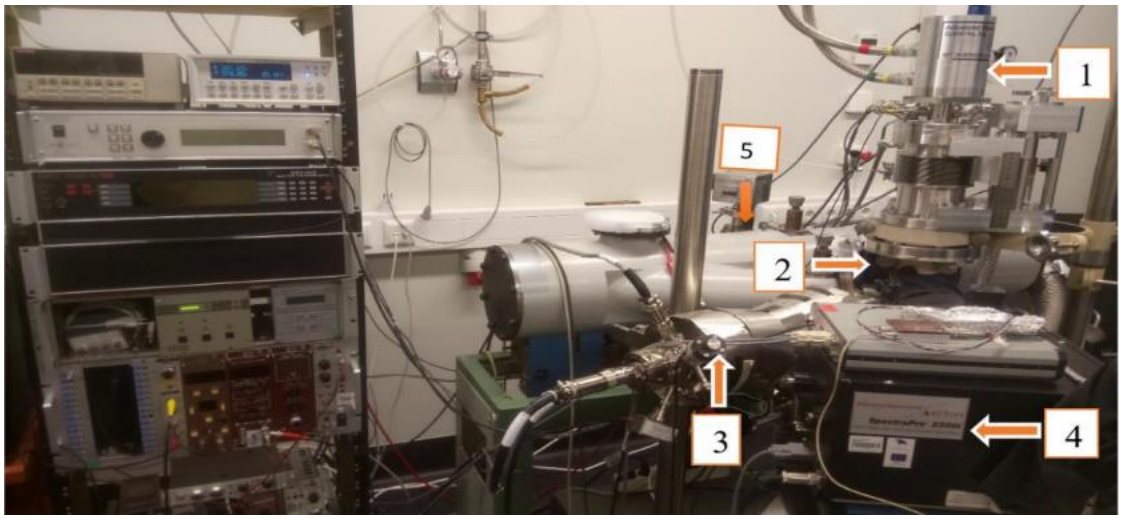

Fig.4: Cathodoluminescence setup. The components of the CL setup are designated by numbers on the photo. (1) a closed cycle vacuum cryostat (Advanced Research Systems); (2) Vacuum chamber ≈ 10^{-7}Torr; (3) An electron gun (EGG-3101 Kimball Physics); (4) ARC Spectra Pro 2300i spectrometer for the UV-visible range; (5) a home-built VUV monochromator.

3.2: Luminescence setup at the FinEstBeAMS beamline of the MAX IV laboratory

Luminescence emission and excitation studies were executed at FinEstBeAMS, at MAX IV (Lund, Sweden) synchrotron radiation laboratory's 1.5 GeV storage ring. Figure 5 shows illustrative description of FinEstBeAMS beamline, which characterization results have been published recently [28]. An elliptically polarized undulator (EPU) of the APPLE II type that is built in-house is used as a photon source in the UV to soft X-ray range 4.5-1300eV, which is followed by plane grating monochromator- (Follath,2001). A toroidal mirror (M1) that is mounted 12.00m from the center of undulator collimates the beam in horizontal and vertical direction. After M1 two pairs of specific baffles (BAFF) are employed to control monochromator's aperture. The monochromator accommodates internally cooled plane mirror (M2) and three slides for side-cooled plane gratings. Presently, two Au-coated plane gratings are installed (PG1, 600 lines mm^{-1} and PG2, 92 lines mm^{-1}). The designated gratings disseminate coming radiations in a vertical plane and the incidence angle of the M2 mirror lead radiations parallel to the incoming beam. The two toroidal focusing mirrors, M3 emphasized the scattered radiation to the exit slit. Next to the exit slit, each branch line contains higher order suppression unit (HOS), where two optical filters (fused silica, MgF_2) and four thin-film metal filters (In, Sn, Mg, Al) are attached on two linear manipulators. Next ellipsoidal mirror (M4) refocuses the monochromated radiation to the end station in each branch. The beamline deploys a standard MAX IV control system based on IcePAP motion controllers and Tango software packages with Sardana framework [28].

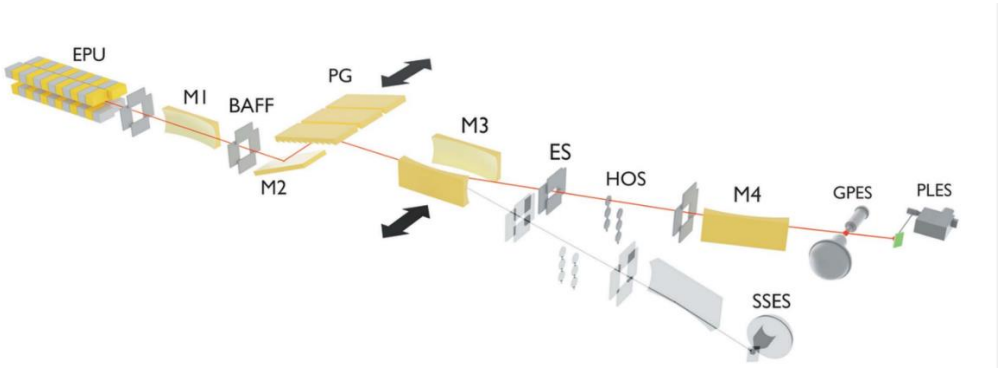

Fig.5: Schematic diagram of the beamline optical system. Where abbreviations are as, EPU – elliptically polarizing undulator, M1–M4 – mirrors, BAFF – baffles, PG – plane grating, ES – exit slit, HOS – higher-order suppressing filters, GPES – gas-phase end station, PLES – photoluminescence end station, and SSES – solid-state end station. [28].

Emission and excitation spectra were recorded via photoluminescence (PL) end station, which is described in [29]. An ellipsoidal mirror focuses the photon beam to a 100x 100 μm spot on the powder samples, mounted on a cold finger of a closed-cycle The cryostat of the photoluminescence end station at FinEstBeAMS [18]. The luminescence of the samples is collected using a fiber optic cable (l ~2 m), which is connected to a 0.3 m Andor Shamrock SR-303i analyzing spectrometer. The spectral analysis of luminescence is carried out either with a Hamamatsu photon counting head H8259-01 covering the spectral range of 200 – 900 nm in the multi-bunch operation mode or with an ultra-fast Hamamatsu R3809U-50 MCP-PMT for time-resolved measurements under single-bunch excitation. Luminescence spectra were corrected for the spectral response of the detection system. Typical spectral resolution used in luminescence measurements was 3 and 6 nm in recording emission and excitation spectra, respectively.

The time resolution is determined by a value of instrumental response function (IRF), which was recorded to be as good as 180 ps. More detailed description of the time-resolved method at FinEstBeAMS can be found in [30].

In order to minimize the influence of higher orders of the excitation light due to higher harmonics of the undulator and higher order transmission of the primary monochromator, a set of thin metallic filters, MgF_2 or fused silica plates were used depending on the excitation energy region studied. The photon flux of the beamline is recorded with an AXUV-100G photodiode for normalizing excitation spectra by to the same amount of incident photons. In the experiments performed a typical slit width of the primary monochromator was set to 150 μm, which corresponds to the excellent spectral resolution better than 4 meV at 10 eV [30].

3.3: Synthesis of $LaPO_4:Pr^{3+}$ Doped Samples

The $LaPO_4:Pr^{3+}$ powder samples for experimental studies were synthesized by our collaboration partners in Münster and Moscow. Micro powders of $LaPO_4:Pr^{3+}$ were synthesized in the group of Prof. Dr. T. Jüstel in the Münster University of Applied Sciences in Germany. Nanopowders of $LaPO_4:Pr^{3+}$ were prepared in the group of Dr. Orlovskii in Prokhorov General Physics Institute, Russian Academy of Sciences in Moscow. Since sample preparation is not the part of current master thesis, therefore here only a brief description is given. Also, the initial characterization of samples (including phase purity by XRD and morphology by TEM studies) was performed in the facilities of the collaborating groups and by their teams.

Micro powder $LaPO_4:Pr^{3+}$ 0.5 % sample

The micro-$LaPO_4:Pr^{3+}$(0.5 %) sample was prepared by a suspension method. Starting materials La_2O_3 and Pr_6O_{11} were mixed with demineralized H_2O, H_3PO_4 was slowly added and suspension was stirred for 24 h. The suspension was dried in a vacuum drying chamber and the obtained powder was milled. Thereafter, the annealing at 1000 °C for 4 h in CO atmosphere was performed. As a result, phase pure (XRD) monazite monoclinic $LaPO_4:Pr^{3+}$ powder was prepared with ~ 4 μm particle size. This micro powder is considered as a representative of bulk material in the current study.

Nano powder $LaPO_4:Pr^{3+}$ samples

Pr^{3+} doped lanthanum phosphate Nano powder samples with different dopant concentrations were synthesized by microwave-hydrothermal treatment technique. Hydrothermal method is specified as a homogeneous or heterogenous reaction at elevated temperature and pressure in the presence of an aqueous solvent [31]. It is most commonly used environment friendly procedure for producing highly crystalline and non-aggregated nanoparticles without addition of toxic and expensive organic surfactant. Under hydrothermal conditions material synthesis require pressure vessels to hold highly corrosive solvents at high temperature and pressure. This technique is also characterized as green chemistry as it requires small amount of energy with no

or minor solid/liquid/gas waste. Additionally, it does not require recovery treatment and this method is highly selective.

Microwave hydrothermal method has been developed in recent years for synthesis of fine powders. It incorporates microwaves for heating using the principle of hydrothermal method. Microwaves have the benefit of penetrating to certain depths of sample and providing uniform heating to inner parts simultaneously. It bars heat conduction resulting from temperature difference, which in turn improves the reaction speed. This technique is employed to produce nanoparticles with narrow particle size distribution and uniform morphology. [32]

The Nano samples $LaPO_4:Pr^{3+}$ with various impurity concentration were prepared analogously to yttrium orthophosphates using synthesized by microwave-hydrothermal treatment as described in [33]. The main phase $LaPO_4:Pr^{3+}$ (0.1 %) nanocrystalline powder has a monoclinic monazite structure. However, the XRD pattern shown in Fig. 6 (a) has an additional reflection at an angle of 14.5 degrees. Energy dispersive analysis showed that, apart from lanthanum, phosphorus, and oxygen, the Nano powder sample contains no other impurities. Consequently, the additional reflection is most likely due to the impurity of the hexagonal modification $LaPO_4$. In the figure, this modification corresponds to the blue color of the XRD pattern. The quantity of this phase is very low and very likely does not influence luminescence spectra. The Figure 6 (b) shows the HR-TEM image of the obtained nanopowders. It consists of fibers with a few hundred nm lengths and few nm in thickness.

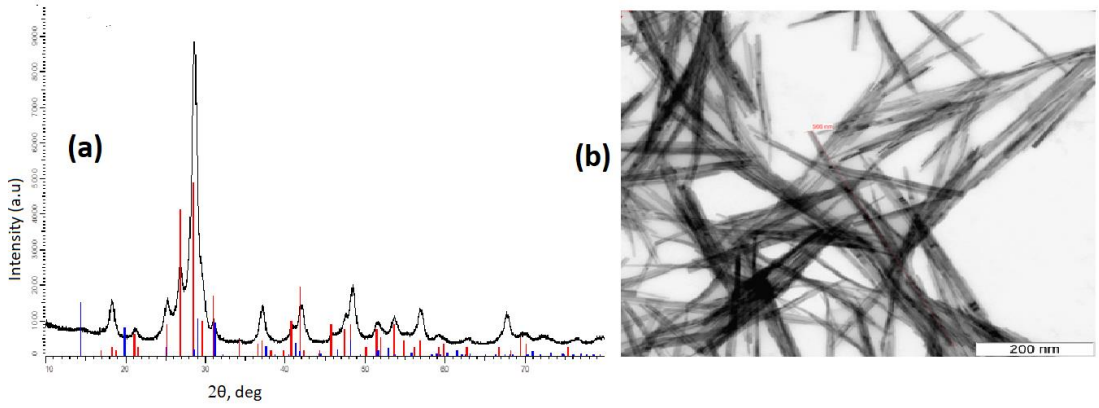

Fig.6: (a) The XRD pattern of $LaPO_4:Pr^{3+}$ (0.1 %) nanocrystalline powder. The red bars show the standard XRD pattern of the main monazite phase (PDF 00-012-0283) and blue bars of hexagonal phase (PDF 01-075-1881). (b) HR-TEM images of the same Nano powder.

4: Results and Discussion

4.1: $LaPO_4$: Pr^{3+}(0.5 %) micro powder sample under $4f^2 \rightarrow 4f^15d^1$ and host excitation

Figure 7 shows 5d-4f emission spectra of $LaPO_4:Pr^{3+}$ 0.5% micro powder sample excited by 6.21 eV photons corresponding to the 4f-5d absorption *i.e.*, intracenter excitation. Spectral features in the 5.8 to 4.4 eV are due $4f^15d^1 \rightarrow {}^3H_{4,5,6}$ and ${}^3F_{2,3}$ interconfigurational transitions. At 295 K there are broad emission bands observed at 3.4 and 2.8 eV (Fig. 7a), which belong transitions from 5d level terminating at ${}^1D_2$ level and ${}^1I_6$, ${}^3P_J$ multiplet of $4f^2$ states in Pr^{3+} ions [12]. Narrow lines at 2.55 and 2.05 eV are assigned to ${}^1D_2$ - ${}^3H_4$ and ${}^3P_0$ - ${}^3H_4$ transitions. As expected the emission bands are spectrally resolved in a better way at lower temperatures (Fig. 7b). At 6.7 K there are some new narrow spectral features appear near 3 eV and redistribution of intensities between different emission bands occurs. All these emission spectra with spectral resolution 4.3 nm were recorded with photomultiplier in the scanning mode, which limits the spectral resolution achieved by a selected slit width and also by step size value providing a number of data points per emission band width.

In order to reveal spectral features with the improved resolution emission spectra were recorded with the Newton DU970P-BVF CCD camera (from Andor) in imaging mode. 200 μm slit width provided very good 2.17 nm (FWHM) spectral resolution. In comparison with the emission spectra shown in Fig. 7 one can see that additonal narrow lines were observed due to pixel size of the CCD camera (16x16 μm) providing up to 1600 data points per a 25.6 mm width of the CCD chip. The narrow line at 4.52 eV is assigned to the $4f^15d^1 - {}^1G_4$ and the group of lines near 3eV is ${}^1S_0$ - ${}^1I_6$ transition, respectively. This is observed in $LaPO_4:Pr^{3+}$ beacuse the highest lying ${}^1S_0$ $4f^2$ state is slightly higher than the lowest $4f^15d^1$ state [12]. Thus, at temperatures below 100 K the both emissions can be observed simultaneously.

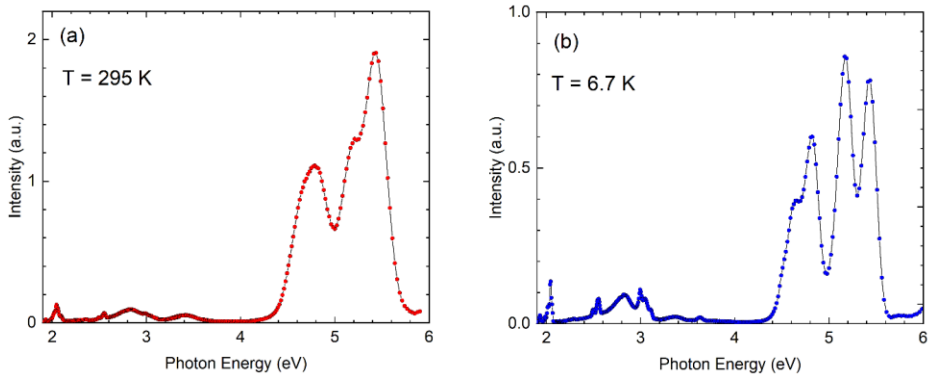

Fig.7: Time-integrated luminescence emission spectra of $LaPO_4:Pr^{3+}$ 0.5% micro powder sample excited by 6.21 eV photons corresponding to $4f^2 \rightarrow 4f^15d^1$ absorption at 295 K (a) and 6.7 K (b).

Fig. 8 (b) shows the decay curves for both emissions (excited by 6.88 eV photons, still resulting in the $4f^2 \rightarrow 4f^15d^1$ excitation) characterised by a single exponential decay τ= 98 ns for $^1S_0$ emission and double exponential for $4f^15d^1$ luminescence τ_1= 11 ns and τ_2= 68 ns, respectively. The second component in decay of $4f^15d^1$ luminescence is due to energy transfer from the higher lying $^1S_0$ $4f^2$ state and rather similar decay constants in several tens of nanoseconds are observed.

The luminescence spectrum (Fig. 8 a) excited by 8.2 eV photons strongly differs from that one excited through $4f^2 \rightarrow 4f^15d^1$ absorption by lower energy photons. Instead of well distinguished $4f^15d^1$ - $^3H_{4,5,6}$ and $^3F_{2,3,4}$ emission bands much broader and smoother spectra were revealed. It resembles to the superposition of Pr^{3+} ions luminescence with the intrinsic self-trapped exciton emission of $LaPO_4$. Although rare earth doped $LaPO_4$ has extensive research history, its intrinsic properties of pure host are practically not investigated. Meunier-Belliard in Ref. [34]. has reported that broad band weak emission peaked at 4.77 eV (260 nm) at 300 K is assigned to the STE emission with the excitation onset at 7.75 eV. The results obtained in the current study depicted in Fig. 8 (a) indicate that under similar excitation conditions the most intense luminescence is revealed at 4.8 eV as broad emission band, which definitely exceeds the width of $4f^15d^1$ to ground state transitions. In addition, decay kinetics of 260 nm emission when exited

above 8 eV undergoes change becoming emission with μs range life-time, which is typical for STE in wide gap materials.

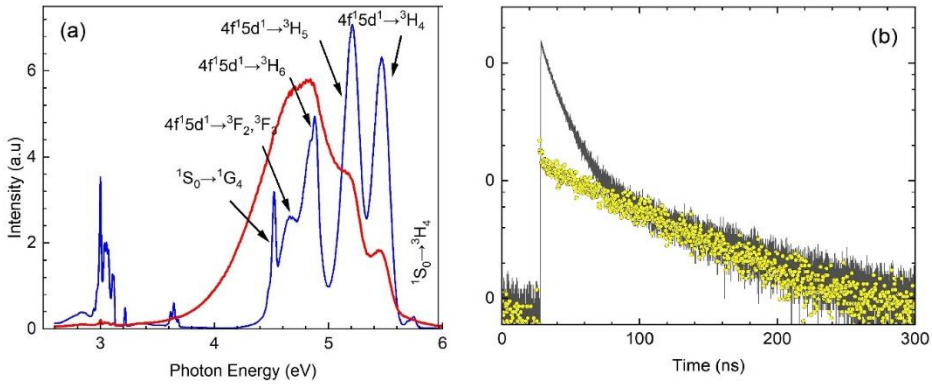

Figure 8: Luminescence emission spectra of $LaPO_4:Pr^{3+}$ 0.5% micro powder sample at 6.7 K excited by 6.44 (blue line) and 8.2 eV (red line) photons recorded by the CCD camera. (b) Decay curves for $4f^15d^1$ - $^3H_6$ emission at 260 nm (black line) and $^1S_0$ - $^1I_6$ emission (symbols) at 406 nm recorded from the same powder at 6.7 K under single bunch operation.

As discussed in Section 2 the highest lying $4f^2$ $^1S_0$ state is energetically located slightly above lowest $4f^15d^1$ state, wherefrom radiative relaxation takes place. At low temperatures, when the potential barrier cannot be overcome, the emissions from both states can take place [10, 12]. Figure 9 demonstrates excitation spectra for the $4f^15d^1$ – $^3H_6$ and $^1S_0$ - $^1I_6$ emissions recorded at 4.77 and 3.05 eV, respectively. The onset $4f^15d^1$ emission is at 5.8 eV followed by a maximum at 6.08, which has been assigned to the $[4f^15d^1]^1$ excited state as labelled in [12]. The onset for the $^1S_0$ - $^1I_6$ emission is shifted to higher energies in agreement with [12] and starts at ~6.0 eV and reaches its first maximum at 6.44 eV, which corresponds to into excitation the $[4f^15d^1]^2$ state, totally 5 of those induced by crystal field splitting of Pr^{3+} 5d states (see Ref. [35] and references therein). The higher energy features in the excitation spectra are located at the same energies, whereas the excitation efficiency distribution varies. This means that both emitting states are populated. A major change occurs at the onset of host absorption above 8 eV, where 260 nm emission either due the $4f^15d^1$ transitions to ground states of Pr^{3+} or self-trapped exciton emission becomes dominant relaxation channel at 6.7 K.

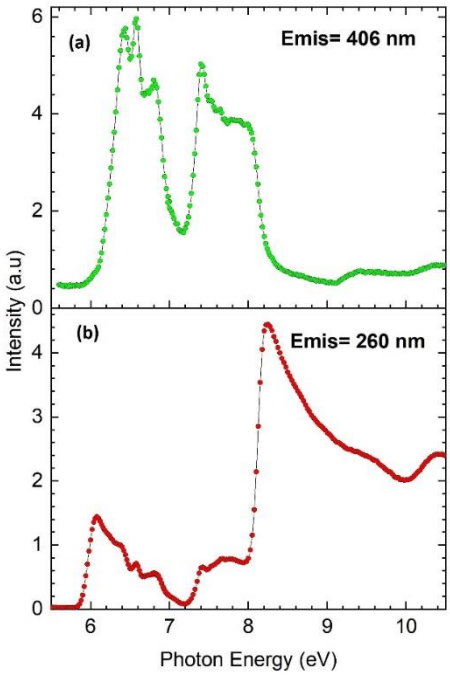

Fig. 9: Excitation spectra for $^1S_0$ - $^1I_6$ emission at 406 nm (a) and $4f^15d^1$ - $^3H_6$ emission at 260 nm (b) recorded from $LaPO_4:Pr^{3+}$ 0.5 % micro powder sample at 6.7 K.

Figure 10 shows the temperature evolution for the 265 nm emission from the $LaPO_4:Pr^{3+}$ 0.5 % micro powder. At temperatures down 250 K, it mostly reflects relaxation processes through the $4f^15d^1 - {}^3H_6$ emission. There are no notable spectral features near intrinsic absorption edge and at energies above 9.5 eV, where formation of electron-hole pairs occurs, the luminescence yields becomes higher than at the direct interconfigurational $4f^2$- $4f^15d^1$ excitation. Starting from 200 K the excitonic peak at 8.2 eV becomes a dominant feature, which exhibits a temperature shift towards higher energies. The results on the studied $LaPO_4:Pr^{3+}$ 0.5 % micro powder sample are in agreement with those reported in [15] for $LaPO_4:Pr^{3+}$ nanoparticles. Timing properties of SR excitation allowed to show that a slow recombination excitation of Pr^{3+} 5d emissions has onset at 8.6 eV, which has been assigned to the energy gap value. The time-integrated excitation spectra shown in Fig. 10 have no distinct features, but having the onset of electron-hole pair formation a few tens of eV above excitonic peak at 8.2 eV us typical for wide gap materials.

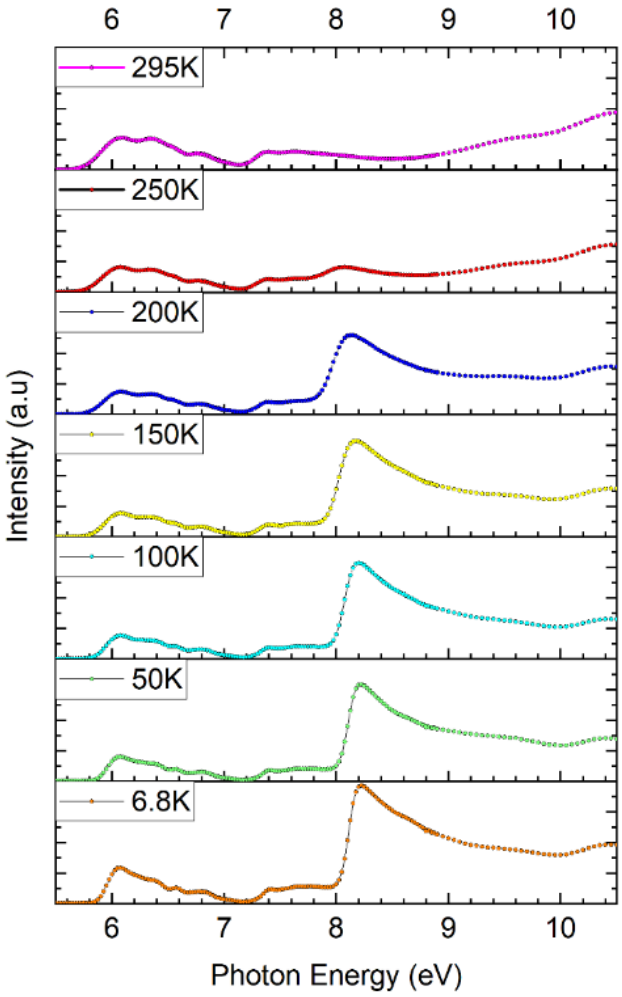

Fig.10: Temperature evolution of excitation spectra of the $LaPO_4:Pr^{3+}$ 0.5 % micro powder sample for the 265 nm emission.

4.2: Cathodoluminescence spectra $LaPO_4:Pr^{3+}$ nanopowders samples

There has been significant interest to study Nano-size $LaPO_4$ doped with Pr [5], Eu and Pr [15], Eu [23, 24], Ce and Tb [25]. It is known that downsizing of host material results in increase of non-radiative processes and decreased luminescence intensity. Also, the decay time may shorten considerably. Figure 11 shows cathodoluminescence spectra of $LaPO_4:Pr^{3+}$ 0.1% Nano powder at various temperatures. The TEM images of this sample consisting of long fibers is shown in Fig. 6b. The length of the fibers is a few hundred nm, whereas the diameter of fibers is a few nm. Thus, the aspect ratio of such studied fibers is rather high 100:1. The quality (signal to noise ratio)

of the emission spectra indicates the nanopowders have significantly lower luminescence intensity in comparison with the micro powder samples discussed in previous sections. This also means that one cannot expect such precision in identification of spectral features, which is typical for well-emitting micro powders. 10 keV electron beam is non-selective excitation, which in the sample excites all kind luminescence centers, independently of their origin. The two distinct peaks with maxima at 5.39 and 4.74 eV are due $4f^15d^1$ - $^3H_{4,5,6}$ and $^3F_{2,3}$ interconfigurational transitions in Nano powder at 295 K. At 5.5 K the luminescence intensity is increased and in the first peak there is a visible structure assigned to transitions terminating in the $^3H_{4,5}$ ground states. The structureless peak at 4.74 eV is mostly due to radiative decay of STE with a contribution from the $4f^15d^1$ - $^3H_6$,$^3F_2$ transitions of Pr^{3+} ion. Namely, at 295 K the luminescence spectra of the bulk Pr^{3+} doped $LaPO_4$ consists of following three emission bands corresponding to electronic transitions: 4f5d→$^3H_4$ (5.4eV / 227nm), 4f5d→$^3H_5$ (5.2eV / 236nm) and 4f5d→$^3H_6$,$^3F_{4,3,2}$(4.8eV / 256nm), (5.4eV / 227nm) [12] and the corresponding values for Nano samples are in general agreement with those as reported in [15].At 2.05 eV there is Pr^{3+} $4f^2$ transition $^1D_2$ – $^3H_4$ clearly visible like micro powder samples (see Fig. 7). Between this narrow emission lines and emission bands in UV, there is always continuous structureless emission band extending from 4.2 to 2.1 eV. There is no obvious correlation with known emission bands from bulk Pr doped $LaPO_4$. It is tentatively assigned to spectral features arising from irregular nanofibers itself, which may include defects, perturbed emission canters near surfaces, etc. The nature of this broad band emission requires further investigation to reveal its origin. While comparing data recorded in Lund using synchrotron radiation excitation and cathodoluminescence spectra acquired in Tartu, data analysis showed that the spectra corrected for spectral sensitivity according function available at both setups have some differences: It is not surprising because obtaining such correction functions is not trivial from the experimental point of view. Data of this thesis work suggests that the corrected cathodoluminescence spectra may have some discrepancy in the lower photon energy range below 2.5 eV. This problem cannot be addressed in the framework of current study, but it has to be revaluated in the further development of cathodoluminescence setup in near future.

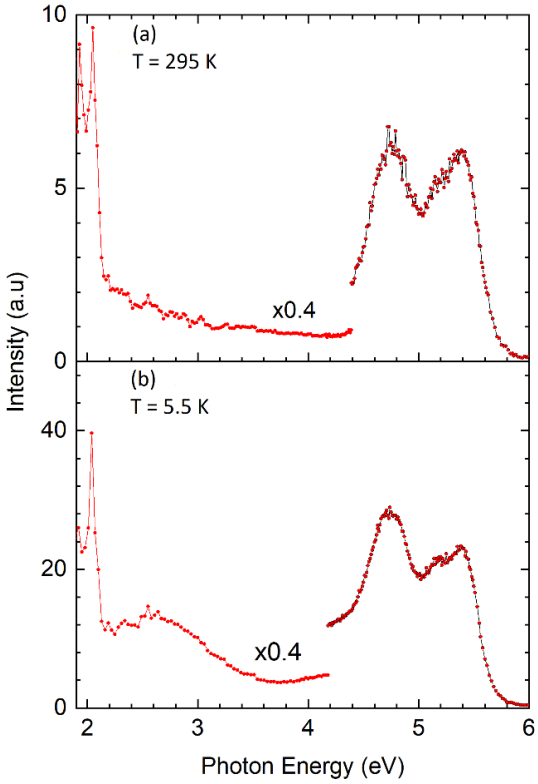

Figure 11. Cathodoluminescence spectra of $LaPO_4:Pr^{3+}$ 0.1% Nano powder at 295 K (a) and 5.5 K (b), excited by 10 keV electron beam. The typical length of fibers is a few hundred nm and thickness of ~ a few nm (see Fig. 6b).

Figure 12 shows cathodoluminescence spectra of $LaPO_4$ Nano powder with higher 1 % Pr^{3+} concentration at 296 (a) and 5.5 (b) K prepared by microwave assisted hydrothermal synthesis. Panel (c) depicts the TEM images of the fibers with 50 nm length and a few nm thicknesses. This Nano powder consists of more symmetric fibers with the reduced aspect ratio than the spectroscopy of the sample discussed just before (data shown in Fig. 11 and Fig 6b).

At 296 K, analogously to the previous Nano sample the luminescence spectra of Pr^{3+} ion consists of doublet at 5.37 and 5.19 and 4.75 eV which are assigned to the $4f^15d^1$ - $^3H_{4,5,6}$ and $^3F_{2,3}$ interconfigurational transitions. At low temperatures at 5.5 K it is expected that intense broad band STE emission gives the strongest contribution to the emission band at 4.7 eV. overlapping with the Pr^{3+} 5d-4f transitions. Again, there is Pr^{3+} $4f^2$ transition $^1D_2$ – $^3H_4$ revealed at 2.05 eV together with structureless luminescence in the range of from 4.2 with rising intensity towards 2.1 eV. The intensity increase starting from 2.8 eV towards low energies is a bit unusual and can be related to the issues with correction function as discussed before.

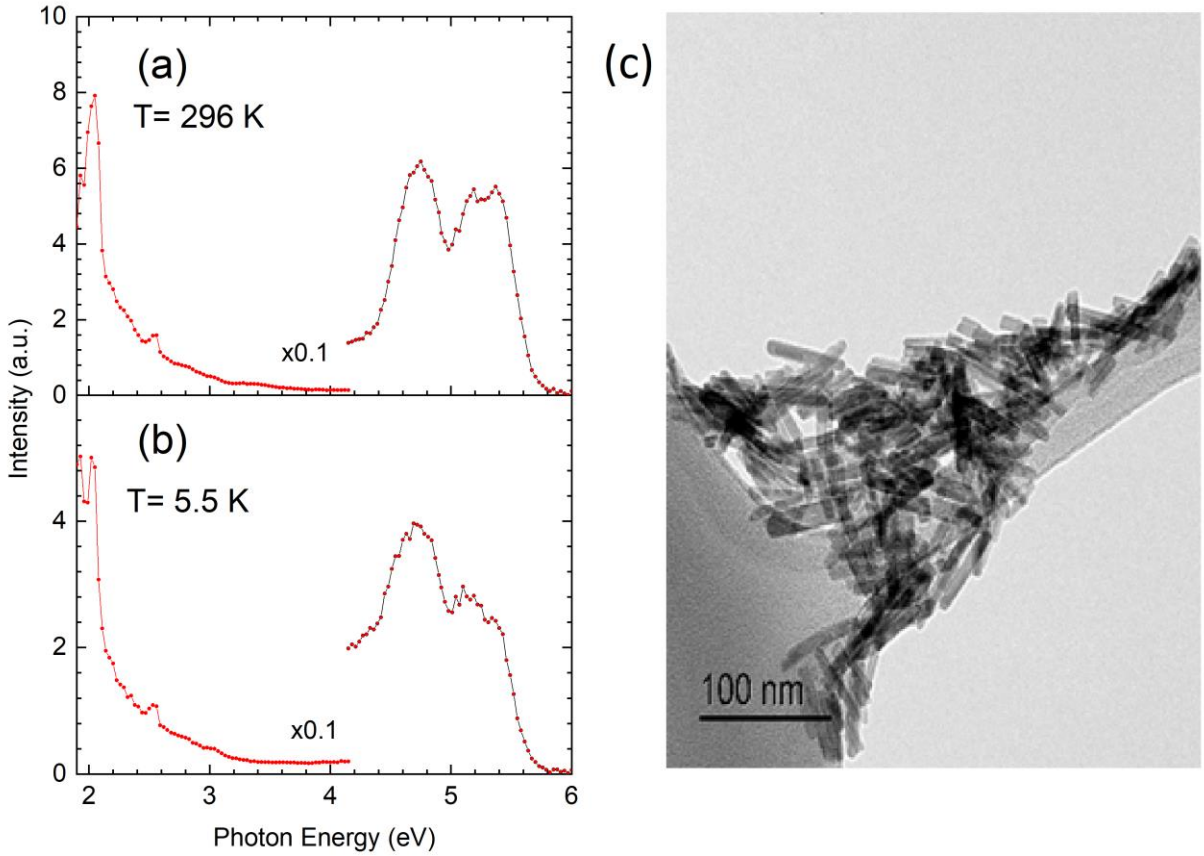

Fig. 12: Cathodoluminescence spectra of $LaPO_4:Pr^{3+}$ 1% at 296 (a) and 5.5 K (b). The typical length of fibers is 50 nm and thickness of ~ a few nm as can be seen in the panel (c) where a TEM image of nanofibers is shown.

Figure 13 shows cathodoluminescence spectra of $LaPO_4$ nanopowders with higher 1 % Pr^{3+} concentration at 296 (a) and 5.5 (b) K prepared by microwave assisted hydrothermal synthesis. Panel (c) depicts the TEM images of the fibers with 40 nm length and a few nm thicknesses. This nanopowders is morphology wise rather close to the previous sample, but for some obvious reasons exhibited better intensity of luminescence as can be seen from the signal to noise ratio of the spectra presented in Fig. 13. (a). The assignment of the observed emissions is analogous one to the previous samples studied by cathodoluminescence. It is a bit surprising that UV bands at low temperatures have less expressed features than at room temperature. The low energy part of the spectrum has a similar rise towards the 2 eV because of the same reasons discussed above.

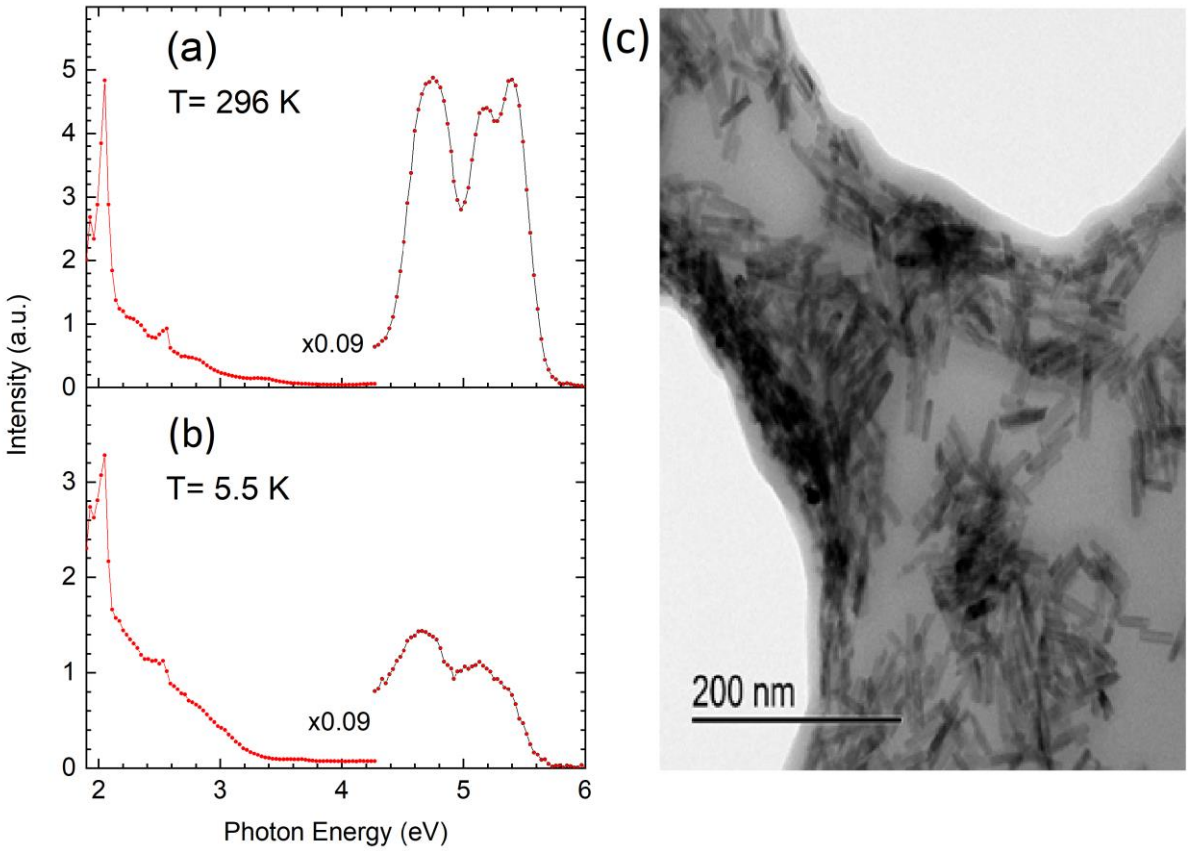

Fig.13: Cathodoluminescence spectra of $LaPO_4:Pr^{3+}$ 1% at 296 K and 5.5 K. The typical length of fibers is 40 nm and thickness of~ a few nm as can be seen in the panel (c) where a TEM image of nanofibers is shown.

The luminescence spectra for the smallest fibers with 20 nm length in average and thickness of ~ a few nm is shown in Fig. 14 (a) for 296 K and 5.5 K (b). Despite of the smallest size cathodoluminescence spectra of these fibers have a good quality and all spectral features as discussed for other nanopowders are revealed. Their interpretation is in line with above presented arguments and would not be repeated here. It is worth of mentioning that luminescence intensity increase towards the lower photon energies may have some dependence on the fiber size. In the room temperature the Pr^{3+} $4f^2$ transition $^1D_2 - {}^3H_4$ at 2.05 eV visible as narrow line is practically growing out of this increasing broad emission band. It can be tentatively interpreted as increased luminescence scattering due to smaller size of fibres (Fig. 14 c).

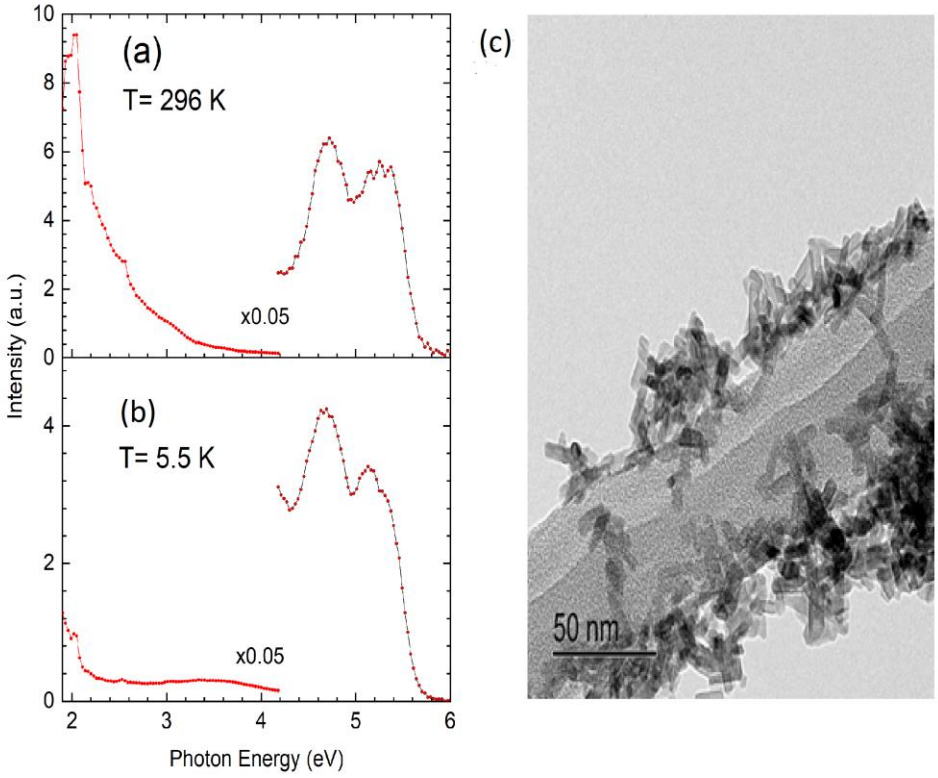

Fig.14: Cathodoluminescence spectra of $LaPO_4:Pr^{3+}$ 1% at 296 K and 5.5 K The typical length of fibres are 20 nm and thickness of ~ a few nm as can be seen in the panel (c) where a TEM image of nanofibers is shown.

In this section it has been shown that all synthesized nanopowders emit expected luminescence in the UV C spectral range. The luminescence intensity on nanofibers is considerably smaller in comparison of bulk materials. Due to several unfortunate circumstances only nanopowders were studied using cathodoluminescence spectroscopy and the study of micro powder samples will be performed in future. All nanopowders have a structureless emission band in the visible region tentatively assigned to the imperfections of nanopowders to be studied beyond this work.

4.3: Luminescence processes in $LaPO_4:Pr^{3+}$ micro and nanopowders under synchrotron radiation excitation

In order to exploit nanopowders as potential scintillators their properties in the operation conditions should be evaluated. In scintillation process there are several stages, which influence their performance. As discussed in the literature review the multiplication processes of electronic excitations are extremely important because this defines how many secondary excitations are produced at the end of process. Also, these created excitations with low kinetic energy participate in the energy transfer processes, which finally populate the luminescence centre i.e., Pr^{3+} ion in context of this thesis. Storage rings generating synchrotron radiation are convenient tuneable light sources providing photons in wide energy range. In order to investigate above mentioned energy transfer processes and formation of secondary excitations by photons in the VUV range the low energy beamlines (4.5-50 eV) like FinEstBeAMS at MAX IV Lab (Lund, Sweden) are especially useful. The experimental setups cover all important energy range relevant to the final stage of the scintillation. It has been shown that in studies of bulk and nanomaterials doped with rare earth ions [15,25, 34, 35] and pure and doped wide gap crystals [13,14] the luminescence spectroscopy under VUV excitation is an indispensable tool. Thus, this was ground to apply spectroscopy under synchrotron radiation excitation in studies of luminescence properties of $LaPO_4$: Pr^{3+} nanopowders and micro powders at low temperatures.

Emission spectra of $LaPO_4:Pr^{3+}$ 0.1 % Nano powder at 6.7 K excited by photons with various energies are depicted in Figure 15. The panel (a) shows the emission spectrum recorded under excitation 6.7 eV photons, which corresponds to intraconfigurational $4f^2 \rightarrow 4f^15d^1$ absorption of Pr^{3+} ions. In the UV range there are there spectral features revealed at 5.39. 5.12 and 4.76 eV. The first two peaks can be related to the $4f^15d^1 \rightarrow {}^3H_4, {}^3H_5$ transitions and the third one to the ${}^3F_{2,3}$ state. This observation agrees with cathodoluminescence spectra of the same sample at 295 K as presented in Fig. 11 (a). In the visible spectral range there is a broad emission band with a maximum at 3.1 eV. In comparison with the cathodoluminescence spectra in Fig. 11 (a, b), this band has more regular shape and it tentatively supports the proposed idea of its origin from the imperfections in nanopowders.

Higher energy 8.22 eV photons cause the formation of intrinsic excitations, excitons in $LaPO_4$ as demonstrated with the excitation spectra in Fig. 10. This is also clearly revealed in Fig. 15 (b), where the dominating emission band is due to self-trapped excitons peaked at 4.7 eV. In the visible range a weak emission of "imperfections" is detected at 3.1 eV together with the $4f^2\ {}^1D_2 - {}^3H_4$ transitions at 2.05 eV. This is an evidence of energy transfer by excitonic mechanism, where created excitons excite other luminescence centres.

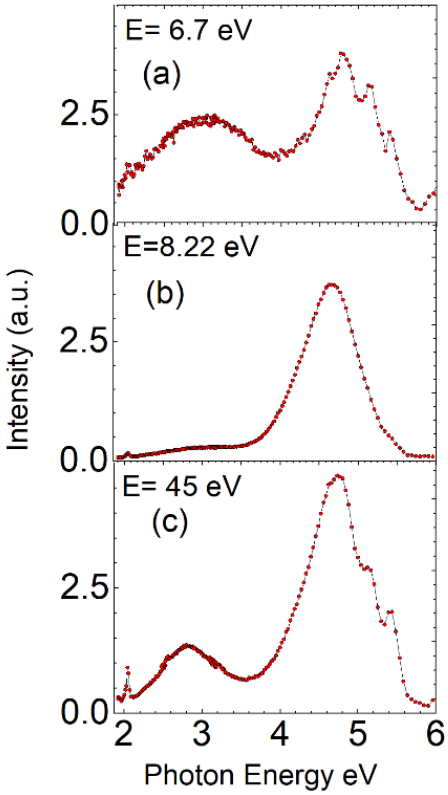

Fig.15: Emission spectra of $LaPO_4:Pr^{3+}$ 0.1 % Nano powder at 6.7 K under excitation by (a) 6.7 eV, (b) 8.22 eV and (c) 45 eV photons. The typical length of fibers is a few hundred nm and thickness of ~ a few nm (see Fig. 6b).

Rather high-energy 45 eV photons exceed the energy gap E_g value 8.6 eV in $LaPO_4$ [15] more than 5 times. Such excitation conditions model the scintillation process because of formation several electronic excitations (either excitons or electron-hole pairs) after absorption of one photon. Secondary excitations are able to transfer energy to the luminescence centres connected with Pr^{3+} ions because 5d-4f emission were revealed in UV range and $4f^2\ ^1D_2 - {}^3H_4$ transitions at 2.05 eV as can be seen in Fig. 15 (c). The observation of the broad emission with maximum at 2.8 eV confirms that this emission can be excited well through host absorption. The maximum of the broad emission band is shifted 0.3 eV towards the lower energies in comparison to the 6.7 eV excitation. This observation indicates that this broad emission band has non-elementary nature with contribution of a few kind of imperfections in nanopowders. The excitation spectra for 4.68 eV and 2.85 eV emissions recorded from the studied micro and nanopowders at 6.7 K are depicted in Fig. 16. The analysis the excitation spectrum for 4.68 eV emission is not trivial because depending on the excitation energy range either the 5d-4f emissions of Pr^{3+} ion (Fig. 15 a) can be excited as it occurs up to 8 eV or the self-trapped exciton emission is the dominating in luminescence (at photon energies > 8 eV, see Fig. 15 b). At higher energies (Fig. 15 c), there is always some contribution from the Pr^{3+}5d-4f luminescence, but self-trapped exciton emission is the strongest. Different radiative relaxation processes contribute to the formation of the excitation spectrum while monitoring single photon energy as shown in Fig. 16 (a). The broad band 2.8 eV emission in also assigned to the 5d transitions to the $^1I_6$, ^3P_J multiplet of $4f^2$ states in Pr^{3+} ions in the micro powders. Thus, the excitation spectra of both 2.8 and 4.68 eV emissions well characterize absorption to the lower $4f^2 \rightarrow 4f^15d^1$ states of Pr^{3+} ions in the region of 5.8 -7 eV, which are followed by absorption to the higher crystal field split 5d states in the range up to 8 eV (see Fig. 16 (a) and (c)). The obtained result, where the presence of spectral features

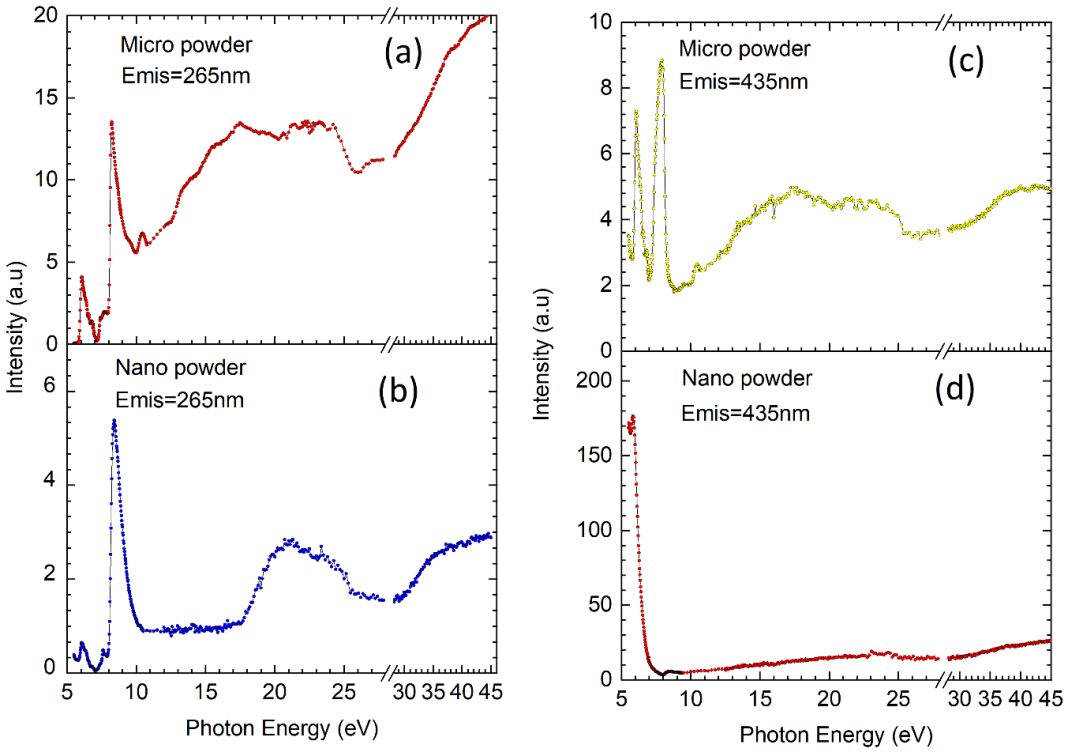

Fig.16: Excitation spectra recorded for 265 nm (4.68 eV) (a, b) and 435 emission (2.85 eV) (c, d) from $LaPO_4:Pr^{3+}$ 0.5 % micro powder (a, c) and $LaPO_4:Pr^{3+}$ 0.1 % Nano powder (b, d) at 6.7 K.

can be explained by the split 5d states, is in a good agreement with the excitation spectrum for the $^1S_0$ emission at 406 nm exhibiting analogous behaviour in the energy range up to 8.2 eV as shown in Fig. 9 (a). Van Pieterson *et al.,* have studied the $4f^2 \rightarrow 4f^15d^1$ excitations of Pr^{3+} ion in YPO_4 by theoretical methods and compared with the experimental excitation spectra in [35]. In this study, it was shown that the onset of such 5d transitions is at 5.39 eV in YPO_4, whereas the higher 5d states result in formation of the highest energy excitation band at 7.75 eV. The experimental observations are in agreement with the energy level and intensity calculations performed by authors of this publication. The host absorption of YPO_4 starts near 8.37 eV being energy wise in the same range as the corresponding region in $LaPO_4$. Ref.35 with findings for Pr^{3+} ions in phosphate host supports our hypothesis that the excitation bands observed up to 8 eV in $LaPO_4:Pr^{3+}$ mainly contribute through $4f^2 \rightarrow 4f^15d^1$ absorption of Pr^{3+}, whereas some absorption just below the exciton band edge at 8.2 eV can be partly introduced by near defect and impurity states.

The 2.85 eV emission in Nano samples has the main excitation peak at 5.8 eV, which is just below the onset of $4f^2 \rightarrow 4f^15d^1$ excitation bands (Fig. 16 (d)). This indicates that the origin of this luminescence centre can be related to the defects *i.e.,* imperfections, which compete with absorption of other impurity centres intentionally introduced like Pr^{3+} ions. After its main excitation peak at 5.8 eV and in the range of host absorption above 8.2 eV, the 2.85 eV emission is excited with rather low efficiency and practically without any dependence on the excitation energy has depicted in Fig. 16 (d). These centres related to the imperfections in nanomaterials are not excited via energy transfer processes of elementary excitations created in the host material.

For scintillator research the most interesting is the behaviour of fast emissions exploited in scintillation in the region host absorption and it will be discussed in this paragraph. Fig 16. (a) depicts the excitation spectrum for 4.68 eV, which is mostly due to the self-trapped emission when excited in intrinsic absorption region. The excitonic peak at 8.2 eV has high intensity followed by a valley with minimum at 10 eV and the intensity of excitation above 18 eV is at the comparable level with that at 8.2 eV. The modulations in the excitation spectra are introduced by near-surface losses introduced by diffusion of electronic excitations to the sample surface and their non-radiative decay introducing minima in the excitation spectra. [36] This is also a reason for the appearance of the deep minimum in 10 – 12 eV region as can be seen in Fig 16 (a) and (c). Above 18 eV the multiplication processes with formation of two electron hole pairs are expected because of the E_g=8.6 eV [15] and the corresponding threshold is above $2E_g \approx 17.2$ eV. The next significant intensity increase occurs above 30 eV and this can be related to the formation of three electron hole pairs. It is obvious that these onsets do not occur exactly at $2E_g$ or $3E_g$ values because energy spent by hot photoelectron in the scattering process is divided between secondary electrons and holes, which gain a certain kinetic energy [13]. Therefore, hot photoelectron has to exceed $2E_g$ or $3E_g$ values and the excitation intensity increase occurs above that threshold a few eV higher. The excitation spectrum for 4.68 eV shown in Fig. 16 (a) does not answer unambiguously whether either the self-trapped excitons are created or Pr^{3+} ions emit 5d-4f luminescence because both contribute to this emission band.

As discussed before the 2.85 eV luminescence can be assigned to 5d transitions, thus the excitation spectrum shown in Fig. 16 (c) directly probes share of Pr^{3+} emissions excited in intrinsic absorption. It is important to point out that the two low energy excitation peaks at 6.1 and 7.9 eV are located outside the intrinsic absorption of $LaPO_4$. Moreover, in this spectrum there is no excitation peak associated with excitonic absorption at 8.2 eV, which means that the behaviour of this excitation spectrum reflects how the 5d states are populated at higher photon energies in the region multiplication of electronic excitations. The shape of excitation spectra for 2.85 eV emission resembles to that for 4.68 eV emission in the energy range from 10 to 45 eV as shown in Fig. 16 (c) and (a), respectively. The excitation intensity level for 2.85 eV emission is about the half of that when applying direct interconfigurational $4f^2 \rightarrow 4f^15d^1$ excitation at 6.1 and 7.9 eV. This suggests that more steep intensity increase observed for 4.68 eV emission primarily due to self-trapped exciton emission. A tentative general conclusion can be drawn that multiplication processes result in more efficient production of secondary excitons and electron hole pairs, but efficiency of energy transfer processes exciting Pr^{3+} ions is not so high under such conditions. The excitation efficiency is practically constant for Pr^{3+} 5d-4f luminescence in the studied energy range (15-45 eV) as depicted in Fig. 16 (c). Thus, the process of multiplication of electronic excitation does not contribute enhance the excitation Pr^{3+} 5d-4f luminescence.

The excitation for 4.68 eV emission from Nano sample is shown in Fig. 16 (b). It looks rather different from its counterpart recorded from micro sample. Namely, the ratio of excitonic peak intensity to the first $4f^2 \rightarrow 4f^15d^1$ excitation at 6.1 eV is much higher in the Nano sample. In turn, it means that likely generation of secondary excitations resulting in STE luminescence is observed in a better way. Indeed, above the excitonic peak at 8.2 eV there is rather flat spectral region up to 18 eV. It is followed by broad band extending from 18 to 25 eV. The next onset of intensity increase is at 30 eV like in the micro powder sample. The onset at 18 eV is assigned to the secondary electron – hole pair creation in $LaPO_4$ nanopowders. This onset is surprisingly well-pronounced, probably due to reduced contribution from the Pr^{3+} 5d-4f luminescence in the UV emission band. The onset identified has a higher value than 17 eV reported in [15]. The reasons for such discrepancy need further research.

5: Summary

The main goal of the present Master Thesis was to investigate potential scintillation materials, which would help to increase the efficiency of radiation therapy for cancer treatment via emitting UV-C locally in patient's tissue. For this purpose, the relaxation processes of electronic excitations in Pr^{3+} doped $LaPO_4$ micro- and nanopowders, synthesized at the collaboration partners, were investigated using cathodoluminescence and photoluminescence. Pr^{3+} doped $LaPO_4$ is well suited scintillator material because of UV-C emissions provide photons with proper energies for cancer therapy. The luminescence properties of prepared $LaPO_4:Pr^{3+}$ nanoparticles were compared with micro powders which represent behaviour of the substance in bulk form. Taking advantage from high quality synchrotron radiation excitation in VUV some intrinsic properties of studied materials were evaluated using luminescence spectroscopy in MAX IV Lab. Cathodoluminescence results were analysed taking into account the morphology of Nano samples obtained by transmission electron microscopy. The following results were obtained as formulated below.

Using synchrotron radiation in the VUV range it was shown that photons > 5.8 eV cause $4f^2 \rightarrow 4f^15d^1$ excitation which results population of 5d states of Pr^{3+} ion decaying radiatively due to the $4f^15d^1 \rightarrow {}^3H_{4,5,6}$ and ${}^3F_{2,3}$ interconfigurational transitions spectrally located from 5.8 to 4.4 eV. These dominant emission bands in the UV-C spectral range are useful for cancer treatment. At low temperatures below 100 K also the radiative transitions from highest lying $4f^2$ ${}^1S_0$ level become observable. This is due to the fact there is a potential barrier between lowest lying 5d and ${}^1S_0$ states. It was shown that the excitation onset for ${}^1S_0$ - ${}^1I_6$ emission at 3.05 eV is higher than that of for 5d-4f emissions. The ${}^1S_0$ - ${}^1I_6$ emission is excited starting from the higher lying $[4f^15d^1]^2$ band until exciton absorption peak at 8.2 eV. Also decay kinetics for both emissions was studied in $LaPO_4:Pr^{3+}$ 0.5 % micro powder. Under 6.88 eV photons excitation to the $[4f^15d^1]^2$ the decay of ${}^1S_0$ - ${}^1I_6$ can be approximated by a single exponential function with a decay time τ=98 ns, whereas a double exponential decay was observed for $4f^15d^1$ luminescence τ_1= 11 ns and τ_2=68 ns.

Investigated nanopowders consist of nanofibers with thicknesses of few nm and lengths varying from 20 to a few hundred nanometers. Nanopowders show a strong decrease in luminescence

intensity as expected due to downscaling of studied material. The studied nanopowders have significantly smaller luminescence intensities as compared to micro powder sample, which indicates a need for optimization of the size of nanoparticles in order to apply these in therapy. All studied nanopowders showed luminescence due to $4f^15d^1 \rightarrow {}^3H_{4,5,6}$ and ${}^3F_{2,3}$ transitions of Pr^{3+} ion. Excitation in the $LaPO_4$ host absorption (> 8.2 eV) resulted in self-trapped exciton luminescence analogously to the studied micro powder samples at low temperatures. The cathodoluminescence studies revealed that in nanopowders independently of their morphology, there is always present broad structureless emission in the UV- visible range from 4 to 2 eV. This is tentatively assigned to the imperfections of nanopowders with different defects, which emit luminescence. There was no well-defined correlation identified between luminescence intensity and nanofiber morphology. Obviously, the nanofibers are too complicated research objects in comparison with spherical nanoparticles.

The final stages of the scintillation process were studied by luminescence spectroscopy under VUV excitation using Estonian Finnish FinEstBeAMS beamline at MAX IV Lab (Lund, Sweden). It was shown that in $LaPO_4$ the multiplication process of electronic excitations has onset at 18 eV, especially well identified in Nano samples. The first onset is related to the formation of two electron-hole pairs and the second one at 30 eV to three such pairs, respectively. The analysis of the excitation spectra for 2.85 eV emission due to 5d-4f transitions to the higher $4f^2$ ground states revealed that the 5d luminescence has a constant yield in the studied energy range 15-45 eV.

To conclude the Master Thesis work, it has been shown that advanced luminescence spectroscopy of materials is valuable method in development of novel functional materials. In this work it has been shown that in downscaling of particle size from micro to nanopowders their properties can be monitored using luminescence spectroscopy. Hopefully, the results of this study contribute to development Nano scintillators for various medical applications.

Kokkuvõte

Magistritöö peaeesmärgiks oli uurida potentsiaalseid stsintillaatormaterjale, mille abil on võimalik suurendada kiiritusteraapia efektiivsust vähiravis viies neid materjalid patsiendi kehasse, kus need kehas lokaliseeritult kiirgavad UV-C piirkonnas mõjutades kasvajarakke. Kasutades katoodluminestsentsi ja footoneid VUV piirkonnas uuriti elektronergastuste relaksatsiooni Pr^{3+} lisandiga $LaPO_4$ mikro ja nanopulbrites, mis sünteesiti koostööpartnerite poolt. Pr^{3+} lisandiga $LaPO_4$ on suurepärane materjal, sest selle UV-C kiirguste footonite energias on väga sobivad vähiraviks. Pr^{3+} lisandiga $LaPO_4$ nanopulbrite luminestsentsomadusi võrreldi mikropulbrite vastavate omadustega ning viimased esindavad materjali omadusi makro (tahkise) olekus. Kasutades suurpärase kvaliteediga sünkrotronkiirgust VUV piirkonnas uuriti $LaPO_4$ põhiaine mõningaid omadusi luminestsentsspektroskoopia meetoditel. Katoodluminestsentsi uuringutulemusi analüüsides võeti arvesse nanopulbrite morfoloogia, mis määrati kindlaks läbivalgustava elektronmikroskoopia abil. Uuritud nanopulbrid koosnevad nanofiibritest, mille paksus on mõned nanomeetrid ja pikkus varieerub 20 kuni mõnesaja nanomeetrini.

Kasutades sünkrotronkiirgust VUV piirkonnas näidati, et footonid energiaga > 5.8 eV ergastavad $4f^2 \rightarrow 4f^15d^1$ ülemineku kaudu Pr^{3+} iooni 5d seisundeid, mis kiirgavad luminestsentsi 5.8 - 4.4 eV piirkonnas ning on seotud Pr^3 iooni $4f^15d^1 \rightarrow {}^3H_{4,5,6}$ ja ${}^3F_{2,3}$ elektronkonfiguratsioonide vaheliste üleminekutega. Need domineerivad kiirgusribad on sobivad vähiteraapiaks, sest kahjustavad selle DNA-d. Madalatel temperatuuridel allpool 100 K muutuvad nähtavaks kiirguslikud üleminekud energeetiliselt kõige kõrgemal asuvast $4f^2\ {}^1S_0$ seisundist. See kiirgus tekib tänu potentsiaali barjäärile madalaima $4f^15d^1$ and ${}^1S_0$ seisundi vahel. Näidati, et ${}^1S_0$ - ${}^1I_6$ 3.05 eV kiirgus ergastub läbi kõrgemate $[4f^15d^1]^2$ seisundite kuni eksiton neeldumisribani 8.2 eV juures. Mõlemate kiirguste (5d ja ${}^1S_0$ seisundist) jaoks uuriti ka luminestsentsi kustumiskineetikat $LaPO_4$:Pr^{3+} 0.5 % mikropulbris. Ergastades 6.88 eV footonitega Pr^{3+} $[4f^15d^1]^2$ seisunditesse, ${}^1S_0$ - ${}^1I_6$ kiirguse kustumine on lähendatav ühe-eksponentsiaalse funktsiooniga kustumisajaga τ=98 ns, kusjuures kahe-eksponendiline lähendus on vajalik $4f^15d^1$ luminestsentsi kirjeldamiseks ning vastavad kustumisajad on τ_1= 11 ns ja τ_2=68 ns.

Uuritud nanopulbrid koosnevad nanofiibritest, mille paksus on mõned nanomeetrid ja pikkus varieerub paarikümnest kuni mõnesaja nanomeetrini. Nanopulbrite luminestsentsi intensiivsus väheneb tugevalt nagu see on oodatud kui vähendada uuritava materjali mõõtmeid. Võrreldes mikropulbriga kiirgusega näitasid kõik uuritud nanopulbrid märkimisväärselt väiksemat luminestsentsi intensiivsust, mis tähendab, et terapeutilisteks rakendusteks on vaja kindlasti nende suurust optimiseerida. Nende nanopulbrite kiirgus on seotud Pr^3 iooni $4f^15d^1 \rightarrow {}^3H_{4,5,6}$ ja ${}^3F_{2,3}$ elektronkonfiguratsioonide vaheliste üleminekutega. Ergastades $LaPO_4$ nanopulbreid nende omaneeldumise piirkonnas (> 8.2 eV) leiti iselõksustunud eksitoni 4.7 eV kiirgus nii nagu mikropulbrites madalatel temperatuuridel. Sõltumatult nanopulbrite morfoloogiast leiti lai struktuuritu kiirgusriba, UV ja nähtavas piirkonnas, ulatudes 4 kuni 2 eV. See on esimeses lähenduses seletatud nanopulbrite multidefektsusega, mis kiirgavad luminestsentsi laias piirkonans. Selge korrelatsioon nanopulbrite morfoloogia ja luminestsentsi vahel puudub. Ilmselt on nanofiibrid liiga keerulised uurimisobjektid võrreldes sfääriliste nanoosakestega.

Stsintillatsioonis aset leidvaid protsesse uuriti FinEstBeAMS kiirekanalil MAX IV Laboris (Lund, Rootsi) kasutades selleks luminestsentsspektroskoopiat VUV ergastusel. Näidati, et elektronergastuste kordistumise protsess algab 18 eV juures kui üks footon tekitab kaks elektron-auk paari. See lävi on eriti hästi näha nanopulbrites. Järgmine luminestsentsi intensiivsuse tõus 30 eV juures on seotud kolme elektron-auk paari tekkega. 2.85 eV luminestsentsi, mis on seotud Pr^{3+} iooni 5d-4f üleminekutega kõrgemal asuvatesse $4f^2$ seisunditesse, ergastusspektri analüüs näitas, et 5d-4f luminestsentsi saagis on praktiliselt konstantne energiapiirkonnas 15-45 eV.

Magistritöö kokkuvõttena võib öelda, et tipptasemel materjalide luminestsentsspektroskoopia on väärtuslik meetod uute funktsionaalsete materjalide arendamisel. Käesoleva uurimusega on näidatud, et materjalide mõõtmete vähendamisel, mikrosuurusest kuni nanomõõtmesse, on võimalik nende omaduste muutusi jälgida luminestsentsspektroskoopia abil. Saadud uuringutulemused Pr^{3+} 5d-4f luminestsentsi kohta on väärtuslik panus nanostsintillaatorite arendamisse erinevate meditsiini rakenduste jaoks.

Acknowledgements

I would like to thank to my supervisor Prof. Marco Kirm for his continuous support, patience and guidance provided during the whole period required to complete the present thesis. I would like to express my gratitude to the Head of Laboratory of Physics of Ionic Crystals Prof. Aleksandr Lushchik for allowing me to carry out my research in this laboratory. I am thankful to Dr Vitali Nagirnyi, Dr. Dmitry Spassky, Dr. Eduard Feldbach and Dr. Ivo Romet for providing knowledge about spectroscopy and technical support in carrying out the measurements at the Institute of Physics, University of Tartu on cathodoluminescence setups.

I am also thankful Prof. Dr. T. Jüstel from the Münster University of Applied Sciences in Germany and Dr. Y. Orlovskii from Prokhorov General Physics Institute, Russian Academy of Sciences in Moscow for providing samples for experimental studies, characterization results of materials and fruitful scientific discussions.

I would like to thank all the personnel from the Laboratory of Physics of Ionic Crystals for friendly atmosphere, support and advices that helped me tremendously throughout the period. I am also very thankful to my family and friends for their comprehensive support during my studies.

References

[1] Bray F, Ferlay J, Soerjomataram I, “Global Cancer Statistics 2018: GLOBOCAN estimates of incidence and mortality worldwide for 36 cancers in 185 countries”, CA Cancer J Clin. 68:394–424(2018).

[2] Delaney G, Jacob S, Featherstone C, Barton M,” The role of radiotherapy in cancer treatment: Estimating optimal utilization from a review of evidence-based clinical guidelines”, Cancer. 104:1129–37(2005).

[3] Srivastava AM, Jennings M, Collins J., “The interconfigurational ($4f^15d^1$ -$4f^2$) luminescence of Pr^{3+} in $LuPO_4$, $K_3Lu\ (PO_4)_2$ and $LiLuSiO_4$”, Optical Materials. 34:1347–52(2012).

[4] Ben Said M, Otaki M, “Development of a DNA-dosimeter system for monitoring the effects of pulsed ultraviolet radiation”, Ann Microbiol. 63:1057–63(2013).

[5] Sara Espinoza, “Deep Ultraviolet Emitting Scintillators for Biomedical Applications: The Hard Way of Downsizing LuPO4:Pr^{3+}”, Part. Part. Syst. Charact. 35, 1800282:1-8(2018).

[6] G. Blasse, B.C. Grabmaier, “Luminescent Materials” pp.25-28.

[7] A. A. Bagatur’yants, I.M. Iskandarova, A.A. Knizhnik, V.S. Mironov, B.V. Potapkin, A.M. Srivastava, and T.J. Sommerer,” Energy level structure of 4f5d states and the Stokes shift in $LaPO_4$: Pr^{3+}: A theoretical study”. PHYSICAL REVIEW B 78, 165125, 1-11 (2008).

[8] MARTINUS H.V. WERTS,” Making sense of lanthanide luminescence”. Science Progress. 88(2), 101–131(2005).

[9] I. Carrasco, K. Bartosiewicz, F. Piccinelli, M. Nikl, and M. Bettinelli,” 5d-4f Radioluminescence in Pr^{3+}-doped $K_3Y_xLu_{1-x}\ (PO_4)_2$” pp.489-490

[10] A.M. Srivastava,” Aspects of Pr^{3+} luminescence in solids”. Journal of Luminescence 169, 445–449(2016)

[11] J. L. Sommerdijk, A. Bril, A. W. de Jager, W. W. Piper, J. A. DeLuca, F. S. Ham, “Two photon luminescence with ultraviolet excitation of trivalent praseodymium” J. Lumin. 8, 341-344(1974).

[12] A.M. Srivastava, A.A. Setlur, H.A. Comanzo, W.W. Beers, P. Schmidt, U. Happek, “The influence of the Pr^{3+} $4f^1$ $5d^1$ configuration on the $^1S_0$ emission efficiency and lifetime in $LaPO_4$” Opt. Mater. 33 292(2011).

[13] A. Lushchik, E. Feldbach, R. Kink, Ch. Lushchik, M. Kirm, and I. Martinson, “Secondary Excitons in Alkali Halide Crystals”, Phys. Rev. B 53 5379-5387(1996).

[14] E. Feldbach, M. Kamada, M. Kirm, A. Lushchik, Ch. Lushchik and I. Martinson. “Direct excitation of impurity ions by hot photoelectrons in wide-gap crystals”, Phys. Rev. B 56 13908-13915(1997).

[15] T. S. Malyy, V. V. Vistovskyy, Z. A. Khapko, et al.,” Recombination luminescence of $LaPO_4$ -Eu and $LaPO_4$ -Pr nanoparticles”. JOURNAL OF APPLIED PHYSICS 113, 224305-1-7(2013)

[16] Christophe DUJARDIN,” Inorganic scintillating materials”. Électronique - Photonique | Optique Photonique EE6347 V1, EE 6 347 – 1-12(2018)

[17] W.M. Yen, S. Shionoya, H. Yamamoto,” Solid-state laser materials” in the handbook of Phosphors, pp.832-838.

[18] S. Espinoza, M.F. Volhard, H. Kätker, H. Jenneboer, A. Uckelmann, M. Haase, M. Müller, M. Purschke, and T. Jüstel,” Deep Ultraviolet Emitting Scintillators for Biomedical Applications: The Hard Way of Downsizing LuPO4: Pr^{3+}”. Part. Syst. Charact., 35, 1800282, 1-8(2018)

[19] M R Neupane, G A Garrett, S Rudin and J W Andzelm,” Phase dependent structural and electronic properties of lanthanum orthophosphate ($LaPO_4$)”. J. Phys.: Condens. Matter 28, 205501 (10pp) (2016)

[20] S.V. Syrotyuk, Ya.M. Chrodolskyy, V.V. Vistovskyy, A.S. Voloshinovskii, A.V. Gektin,” Band structure of $LaPO_4$”. Functional materials 20, 3 373-377(2013)

[21] E. NAKAZAWA and F. SHIGA,” VACUUM ULTRAVIOLET LUMINESCENCE-EXCITATION SPECTRA of RPO_4: Eu^{3+} (R = Y, La, Gd and Lu)”. Journal of Luminescence 15 255—259(1977)

[22] K.C. Mishraa, I. Osterloh, H. Anton, B. Hannebauer, P.C. Schmidt, K.H. Johnson,” First principles investigation of host excitation of $LaPO_4$, La_20_3, and $AlP0_4$”. Journal of Luminescence 72-74 144-145(1997)

[23] L. Yu, H. Songa, S. Lu, Z. Liu, L. Yang, and X. Kong,” Luminescent Properties of $LaPO_4$: Eu Nanoparticles and Nanowires”. J. Phys. Chem. B, 108, 16697-16702 (2004)

[24] J. J. H. A. van Hest, G. A. Blab, H. C. Gerritsen, C. de Mello Donega, and A. Meijerink,” Probing the Influence of Disorder on Lanthanide Luminescence Using Eu-Doped $LaPO_4$ Nanoparticles”. J. Phys. Chem. C, 121, 19373−19382(2017)

[25] V. Pankratova, A. I. Popov, L. Shirmane, A. Kotlov, and C. Feldmann," $LaPO_4$: Ce, Tb and YVO_4: Eu nanophosphors: Luminescence studies in the vacuum ultraviolet spectral range". JOURNAL OF APPLIED PHYSICS 110, 053522 1-7 (2011)

[26] Hiromi Yamashita," XAFS Analysis and Applications to Carbons and Catalysts"," In the handbook of Carbon Alloys: Novel Concepts to Develop Carbon Science and Technology. Pp189-209(2003)

[27] E. Feldbach, E. Tõldsepp, M. Kirm, A. Lushchik, K. Mizohata, and J. Räisänen. "Radiation resistance diagnostics of wide-gap optical materials." Optical Materials 55: 164-167 (2016)

[28] K. Chernenko, A. Kivimaki, R. Parna, W. Wang, R. Sankari, M. Leandersson, H. Tarawneh, V. Pankratov, M. Kook, E. Kukk, L. Reisberg, S. Urpelainen, T. Kaambre, F. Siewert, G. Gwalt, A. Sokolov, S. Lemke, S. Alimov, J. Knedel, O. Kutz, T. Seliger, M. Valden, M. Hirsimaki, M. Kirm and M. Huttula," Performance and characterization of the FinEstBeAMS beamline at the MAX IV Laboratory". J. Synchrotron Rad. 28 1620-1630(2021).

[29] V. Pankratov, R. Pärna, M. Kirm, V. Nagirnyi, E. Nõmmiste, S. Omelkov, S. Vielhauer, K. Chernenko, L. Reisberg, P. Turunen, A. Kivimäki, E. Kukk, M. Valden and M. Huttula, "Progress in development of a new luminescence setup at the FinEstBeAMS beamline of the MAX IV laboratory". Radiation Measurements 121 91-98(2019).

[30] J. Saaring, A. Vanetsev, K. Chernenko, E. Feldbach, I. Kudryavtseva, H. Mändar, R. Pärna, V. Nagirnyi, S. Omelkov, I. Romet, O. Rebane and M. Kirm. "Relaxation of electronic excitations in K2GeF6 studied by means of time-resolved luminescence spectroscopy under VUV and pulsed electron beam excitation". J. Alloys Compd. 883 160916(2021).

[31] Guoming Huang, Chun-Hua Lu, Huang-Hao Yang," MAGNETIC NANOMATERIALS FOR MAGNETIC BIOANALYSIS" in the handbook of," Novel Nanomaterials for biomedical, environmental and energy applications", Pages 89-109(2019,)

[32] Guijun Yang and Soo-Jin Park," Conventional and Microwave Hydrothermal Synthesis and Application of Functional Materials: A Review", Materials , 12(7), 1177(2019)

[33] A.S. Vanetsev, E.V. Samsonova, O.M. Gaitko, K. Keevend, A.V. Popov, U. Mäeorg, H. Mändar, I. Sildos, Yu.V. Orlovskii, "Phase composition and morphology of nanoparticles of yttrium

orthophosphates synthesized by microwave-hydrothermal treatment: The influence of synthetic conditions", Journal of Alloys and Compounds 639 415-421(2015).

[34] Ph. Meunier-Beillard, B. Moine, C. Dujardin, X. Cieren, C. Pedrini, D. Huguenin & V. Archambault, "Exciton trapping in $LaPO_4$ doped with trivalent cerium and/or terbium ions, Radiation Effects and Defects in Solids", 149 25-30 (1999).

[35] L. van Pieterson, M. F. Reid, R. T. Wegh, S. Soverna and A. Meijerink, "$4f^n$- $4f^{n-1}5^d$ transitions of the light lanthanides: Experiment and theory", PHYSICAL REVIEW B, 65 045113(2002).

[36] J. Becker, M. Kirm, V.N. Kolobanov, V.N. Makhov, V.V. Mikhailin, A.N. Vasil'ev and G. Zimmerer, Coexistence of Triplet and Singlet Exciton Emission in Alkaline Earth Fluoride Crystals. in "Excitonic Processes in Condensed Matter" R.T. Williams and W.M. Yen, Editors, PV 98-25, The Electrochemical Society Proceedings Series, Pennington, NJ 415-419(1998).

Appendix

1.Licence

Non-exclusive licence to reproduce the thesis and make the thesis public

I, **Umama Quddusi**

1.grant the University of Tartu a free permit (non-exclusive licence) to
reproduce, for the purpose of preservation, including for adding to the DSpace digital archives until the expiry of the term of copyright, my thesis

Investigation of luminescence properties of Pr^{3+} doped $LaPO_4$ micro- and nanopowders

supervised by **Prof. Marco Kirm.**

2. I grant the University of Tartu a permit to make the thesis specified in point 1 available to the public via the web environment of the University of Tartu, including via the DSpace digital archives, under the Creative Commons licence CC BY NC ND 4.0, which allows, by giving appropriate credit to the author, to reproduce, distribute the work and communicate it to the public, and prohibits the creation of derivative works and any commercial use of the work until the expiry of the term of copyright.

3. I am aware of the fact that the author retains the rights specified in points 1 and 2.

4. I confirm that granting the non-exclusive licence does not infringe other persons' intellectual property rights or rights arising from the personal data protection legislation.

Umama Quddusi

31/05/2022